Anonymous Referee #1

In general, I accept the authors' response to my primary criticism that this work is not relevant until the much larger errors in primary emissions are corrected. Their point that the inclusion of these more realistic techniques for emissions from fertilizer and livestock allow for clearer attribution of remaining errors to other sources is well taken. Also, by including these advances in the adjoint the other errors will be more easily estimated. I appreciate the addition of the SEARCH data comparison. This is compelling evidence that the diurnal behavior is much more realistic.
The plots are still too small but they are now expandable on the computer. The question now is: should figures in journal articles be legible and comprehensible in hard copy form or is it sufficient that they can be expanded on a computer screen? I leave this question for the editors.

Page 18, lines 576-577: I don't understand the reference to Figure 18, upper right. The plot in the upper right in sensitivity to fertilizer rate in April, not sensitivity to soil pH.

We apologize for the misunderstanding. It should be "upper left". See line 583.

Anonymous Referee #3

While the authors have made some useful revisions to the manuscript, I still think there are two important issues that haven't been addressed:
1) By only carrying out model-measurement comparisons with monthly averages, the assessment of the bidirectional flux parameterization is weakened. Essentially, they are only looking at whether it improves the representation of variability at coarse spatial and temporal scales. Their results imply that the parameterization does not improve the model fidelity, but I suspect that may be a result of the scales they chose. This should be discussed, at least.

Thanks for the comments. We have considered the impacts of bi-directional exchange on the diurnal variability of NH_3 surface concentrations at SEARCH sites. However, we only found small changes as the SEARCH site are not dominated by the fertilizer sources.
We now added a paragraph to the conclusion, see line 667. "Moreover, as the in situ measurements used here are limited in space and time, the comparisons between model and measurements only represents the ability of bi-directional parameterization at these specific spatial (100's of km) and temporal (monthly) scales; more pronounced impacts may occur at finer scales."

2) The text accompanying the global maps of model output continues to only specify minimum and/or maximum changes when the majority of the planet has changed very little. Their statement that the median change is very small is not a good argument for only quoting the maximum! Perhaps some

probability distribution functions could accompany the figures to help the reader judge the typical change between model runs.

Thanks for the comments. We did consider distribution functions, but found that since the mean and median did not shift, they did not provide much useful information. However, we agree it is good to mention the aspects of probability distribution, such as the mean, median and standard deviation, which we now mention on line 440 and 473:

"As evident from the figure, the differences in many places throughout the globe are very slight. With positive and negative differences, the global mean and median of the changes are quite small (for example, the mean and median differences in July are -0.02 Gg/month and zero, respectively). However, there are areas where the differences deviate significantly from zero (for example the standard deviation of the difference in July is 3.76 Gg/month in China). We thus focus our discussion on the range of differences in particular regions that are evident from Figure 13."

"Although bi-directional exchange changes NH_3 concentrations slightly throughout the world (mean and median values of the differences are all nearly zero in all three months), significant changes still exist in many places."

Manuscript prepared for Atmos. Chem. Phys.
with version 2014/07/29 7.12 Copernicus papers of the LaTeX class copernicus.cls.
Date: 10 October 2015

Global evaluation of ammonia bi-directional exchange and livestock diurnal variation schemes

Liye Zhu[1], Daven Henze[1], Jesse Bash[2], Gill-Ran Jeong[1,2], Karen Cady-Pereira[3], Mark Shephard[4], Ming Luo[5], Fabien Paulot[6,7], and Shannon Capps[2]

[1]Department of Mechanical Engineering, University of Colorado, Boulder, Colorado, USA.
[2]US Environmental Protection Agency, Research Triangle Park, North Carolina, USA.
[3]Atmospheric and Environmental Research, Inc., Lexington, Massachusetts, USA.
[4]Environment Canada, Toronto, Ontario, Canada.
[5]Jet Propulsion Laboratory, California Institute of Technology Pasadena, CA, USA.
[6]Program in Atmospheric and Oceanic Sciences, Princeton University, Princeton, New Jersey, USA.
[7]Geophysical Fluid Dynamics Laboratory/National Oceanic and Atmospheric Administration, Princeton, New Jersey, USA.

Correspondence to: Daven K. Henze (daven.henze@colorado.edu)

Abstract. Bi-directional air-surface exchange of ammonia (NH_3) has been neglected in many air quality models. In this study, we implement the bi-directional exchange of NH_3 in the GEOS-Chem global chemical transport model. We also introduce an updated diurnal variability scheme for NH_3 livestock emissions and evaluate the recently developed MASAGE_NH_3 bottom up inventory. While updated diurnal variability improves comparison of modeled-to-hourly in situ measurements in the Southeastern US, NH_3 concentrations decrease throughout the globe, up to 17 ppb in India and Southeastern China, with corresponding decreases in aerosol nitrate by up to 7 μg m^{-3}. The ammonium (NH_4^+) soil pool in the bi-directional exchange model largely extends the NH_3 lifetime in the atmosphere. Including bi-directional exchange generally increases NH_3 gross emissions (7.1%) and surface concentrations (up to 3.9 ppb) throughout the globe in July, except in India and Southeastern China. In April and October, it decreases NH_3 gross emissions in the Northern Hemisphere (e.g., 43.6% in April in China) and increases NH_3 gross emissions in the Southern Hemisphere. Bi-directional exchange does not largely impact NH_4^+ wet deposition overall. While bi-directional exchange is fundamentally a better representation of NH_3 emissions from fertilizers, emissions from primary sources are still underestimated and thus significant model biases remain when compared to in situ measurements in the US. The adjoint of bi-directional exchange has also been developed for the GEOS-Chem model and is used to investigate the sensitivity of NH_3 concentrations with respect to soil pH and fertilizer application rate. This study thus lays the groundwork for future inverse modeling studies to more directly constrain these physical processes rather than tuning bulk uni-directional NH_3 emissions.

1 Introduction

Ammonia (NH_3) is an important precursor of particulate matter ($PM_{2.5}$) that harms human health (Reiss et al., 2007; Pope et al., 2009; Crouse et al., 2012) and impacts climate through aerosol and short-lived greenhouse gas concentrations (Langridge et al., 2012). Global emissions of NH_3 have increased by a factor of 2 to 5 since pre-industrial times, and they are projected to continue to rise over the next 100 years (Lamarque et al., 2011; Ciais et al., 2013). NH_3 is an important component of the nitrogen cycle and accounts for a significant fraction of long-range transport (100's of km) of reactive nitrogen (Galloway et al., 2008). Excessive deposition of NH_3 already threatens many sensitive ecosystems (Liu et al., 2013).

Uncertainties in estimates of NH_3 emissions are significant. Surface-level NH_3 measurements have been limited in spatial and temporal coverage, leading to large discrepancies in emissions estimates (Pinder et al., 2006). Additional information from remote sensing observations has been used to gain a better understanding of NH_3 distributions (Clarisse et al., 2009; Shephard et al., 2011; Pinder et al., 2011; Van Damme et al., 2014). These observations have also been used as inverse modeling constraints on NH_3 emissions (Zhu et al., 2013). While this approach leads to improved results regarding the comparison of air quality model estimates to independent surface observations in the US (Zhu et al., 2013), several limitations of this approach were identified. First, model biases in NH_x wet deposition were not reduced. Emission constraints from remote sensing measurements available only once per day were very sensitive to the model's diurnal variation of NH_3 sources. Also, the remote sensing observations used in Zhu et al. (2013) are sparsely distributed, leading to a quantifiable sampling bias. Other inverse modeling studies of NH_3 emissions have been performed using in situ observations, such as aerosol SO_4^{2+} and NO_3^- (Henze et al., 2009), aircraft observations of NH_3 (Schiferl et al., 2014) or wet deposition of NH_4^+ (Paulot et al., 2014). However, these approaches still have disadvantages as they are limited to the small spatiotemporal coverage of available aircraft measurements, or are sensitive to large model biases in HNO_3 (Heald et al., 2012; Zhang et al., 2012) or precipitation Paulot et al. (2014).

The modest success of previous inverse modeling studies suggests that updates to the dynamic and physical processes governing NH_3 are needed in addition to improvements in emissions estimates. Nighttime NH_3 concentrations are consistently overestimated in many air quality models (e.g., GEOS-Chem global chemical transport model and the Community Multiscale Air-Quality (CMAQ)). This may contribute to an overestimate of monthly averaged NH_3 concentration following the assimilation of Tropospheric Emission Spectrometer (TES) observations (Zhu et al., 2013).

Another area in which many air quality models are currently deficient is in treatment of the air-surface exchange of NH_3. Rigorous treatment of the bi-directional flux of NH_3 can substantially impact NH_3 deposition, emission, re-emission and atmospheric lifetime (Sutton et al., 2007). Re-emission of NH_3 from soils can be a significant part of NH_3 sources in some regions. However, this bi-directional exchange mechanism is neglected by many air quality models (e.g., GEOS-Chem).

Several recent studies have begun to include resistance-based bi-directional exchange wherein the NH_3 flux direction is determined by comparing the ambient NH_3 concentration to the NH_3 in-canopy compensation point. Sutton et al. (1998) and Nemitz et al. (2001) began with the air-canopy exchange model and extended the model by including air-soil exchange, but with no soil resistance. Cooter et al. (2010) and Bash et al. (2010) developed and extended the model to include a soil capacitance which assumes that NH_3 and NH_4^+ exist in equilibrium in the soil. This NH_3 bi-directional exchange scheme has been evaluated in a regional air-quality model (CMAQ) by Bash et al. (2013) and Pleim et al. (2013).

Based on these previous studies, investigating the diurnal patterns of NH_3 emissions and bi-directional air-surface exchange is critical for reducing uncertainties in the GEOS-Chem model, which may in turn afford better top-down constraints on NH_3 source distributions and seasonal variations. In this paper, we apply a new diurnal distribution pattern to NH_3 livestock emissions in GEOS-Chem, which is developed based on observations of emissions in the Concentrated Animal Feeding Operation (CAFO) dominated areas in North Carolina (Zhu et al., 2015). We then implement bi-directional exchange of NH_3 in a global chemical transport model – GEOS-Chem – following Pleim et al. (2013), and compare the model to in situ observations. As a first step towards including bi-directional exchange in NH_3 inverse modeling, we also develop the adjoint of bi-directional exchange in GEOS-Chem; this also provides a useful method for quantifying the sensitivities of GEOS-Chem simulations with respect to important parameters in the bi-directional model, such as soil pH and fertilizer (only mineral fertilizer is considered in NH_3 bi-directional exchange) application rate, which are themselves uncertain.

Section 2 describes the model we use in this study. Section 3 introduces the in situ observation networks we use for evaluation. The impacts of implementing the new diurnal variation pattern of NH_3 emissions are presented in section 4. The details of developing bi-directional exchange and its adjoint in GEOS-Chem are described in section 5, followed by the evaluations and adjoint sensitivity analysis in section 6. We present our conclusions in section 7.

2 Methods

2.1 GEOS-Chem

GEOS-Chem is a chemical transport model driven with assimilated meteorology from the Goddard Earth Observing System (GEOS) of the NASA Global Modeling and Assimilation Office (Bey et al., 2001). We use the nested grid of the model (horizontal resolution 1/2 $^\circ\times$ 2/3° ($\sim$ 50 km $\times$ 67 km) over the US and 2$^\circ\times$ 2.5° ($\sim$ 200 km $\times$ 250 km) horizontal resolution for the rest of the world. The year 2008 is simulated with a spin-up period of 3 months. The tropospheric oxidant chemistry simulation in GEOS-Chem includes a detailed ozone-NO_x-hydrocarbon-aerosol chemical mechanism (Bey et al., 2001) coupled with a sulfate-nitrate-ammonia aerosol thermodynamics module described

in Park et al. (2004). The wet deposition scheme of soluble aerosols and gases is described in Liu et al. (2001). The dry deposition of aerosols and gases scheme is based on a resistance-in-series model (Wesely, 1989), updated here to include bi-directional exchange (see Section 5).

Global anthropogenic and natural sources of NH_3 are from the GEIA inventory 1990 (Bouwman et al., 1997). The anthropogenic emissions are updated by the following regional inventories: the 2005 US EPA National Emissions Inventory (NEI) for US, the Criteria Air Contaminants (CAC) inventory for Canada (van Donkelaar et al., 2008), the inventory of Streets et al. (2006) for Asia, and the Co-operative Program for Monitoring and Evaluation of the Long-range Transmission of Air Pollutants in Europe (EMEP) inventory for Europe (Vestreng and Klein, 2002). Monthly biomass burning emissions are from van der Werf et al. (2010), and biofuel emissions are from Yevich and Logan (2003). The anthropogenic emissions inventories described here are only used for base case nested grid model runs over the US. Variants will be explained in the following sections. Table 1 is a summary of various emissions inventories used in different sections.

2.2 GEOS-Chem adjoint model

An adjoint model is an efficient tool for investigating the sensitivity of model estimates with respect to all model parameters simultaneously. This approach has been applied in recent decades in chemical transport models for source analysis of atmospheric tracers (Fisher and Lary, 1995; Elbern et al., 1997) and for constraining emissions of tropospheric chemical species (Elbern et al., 2000). Adjoint models have also been used in air quality model sensitivity studies (e.g., Martien and Harley, 2006). The adjoint of GEOS-Chem is fully described and validated in Henze et al. (2007). It has been used for data assimilation using in situ observations (e.g., Henze et al., 2009; Paulot et al., 2014) and remote sensing observations (e.g., Kopacz et al., 2010; Zhu et al., 2013; Xu et al., 2013). In this paper, we develop the adjoint of bi-directional exchange and we use this adjoint model to investigate the sensitivity of modeled NH_3 with respect to soil pH and fertilizer application rate.

3 Observations

3.1 Surface measurements

We use surface observations of NH_3 and wet deposited NH_4^+ from several networks to evaluate model estimates.

The SouthEastern Aerosol Research and Characterization (SEARCH) network contains monitoring stations throughout the Southeast US. The SEARCH network provides different sampling frequencies, such as daily, 3-day, 6-day, 1-min, 5-min and hourly, at different sites. Three of the monitoring stations (Oak Grove, MS, Jefferson Street, GA, and Yorkville, GA) provide 5-min long surface NH_3 observations. In order to see the diurnal variations, we convert the 5-min long observations to be hourly average NH_3 concentration for each of these three sites in July 2008. We then

average the hourly observations of these three sites to compare with the modeled results of corresponding sites.

The Ammonia Monitoring Network (AMoN) of National Atmospheric Deposition Program (NADP) contains 21 sites across the US with two-week long sample accumulation (Puchalski et al., 2011). We average the two-week long observations from November 2007 through June 2010 to monthly NH_3 concentrations. The Interagency Monitoring of Protected Visual Environments (IMPROVE) network (Malm et al., 2004) consists of more than 200 sites in the continental US which collect $PM_{2.5}$ particles over 24 hours every third day. We use monthly average sulfate and nitrate aerosols concentrations.

We use wet NH_4^+ deposition observations from several monitoring networks around the world. The NADP National Trends Network (NTN) (http://nadp.sws.uiuc.edu/NTN) contains more than 200 sites in US which are predominately located in rural areas. It provides wet deposition observations of ammonium with week-long sample accumulation. The Canadian Air and Precipitation Monitoring Network (CAPMoN) (http://www.on.ec.gc.ca/natchem) contains about 26 sites which are predominately located in Central and Eastern Canada with 24-hour integrated sample times. The European Monitoring and Evaluation Program (EMEP) (http://www.nilu.no/projects/ccc/emepdata.html) contains about 70 sites which are predominately located away from local emission sources. It has daily, weekly, and bi-weekly observations of ammonium available in different sites. The Acid Deposition Monitoring Network in East Asia (EANET) (http://www.eanet.asia/product) contains 54 sites (21 urban, 13 rural, and 20 remote sites) with monthly observations of wet deposition of ammonium. We only use nonurban sites ($\sim$30) of EANET to avoid large local emission sources influences. We convert the daily/weekly/bi-weekly observations to monthly average NH_4^+ concentration in 2008.

4 Diurnal variability of ammonia livestock emission

4.1 Development of new diurnal distribution scheme

Simulated NH_3 surface concentrations in GEOS-Chem are significantly overestimated at nighttime compared to hourly observations from the SEARCH network (Zhu et al., 2013). The standard NH_3 emissions in GEOS-Chem are evenly distributed throughout the 24 hours of each day of the month, as indicated by the blue line in Figure 1. That the simulated NH_3 emissions do not have any diurnal variation is a likely explanation for this discrepancy with hourly observation. Thus, a new diurnal distribution scheme for NH_3 livestock emissions has been developed in CMAQ (Zhu et al., 2015). Here we implement this algorithm in GEOS-Chem. The hourly NH_3 livestock emission, $E_h(t)$, is calculated from the monthly total emission, E_m, as

$$E_h(t) = E_m N_{met}(t), \quad (1)$$

where $N_{met}(t)$ is the hourly fraction of the NH_3 livestock emission during the month. This depends on the aerodynamic resistance, R_a [$s^{-1}m$], and surface temperature, T [K],

$$N_{met}(t) = \frac{H(t)/R_a(t)}{\sum_{t=1}^{n}(H(t)/R_a(t))}, \quad (2)$$

where n is the number of hours in a month, t is the time during the month, from 1 to n, and $H(t)$ is the Henry's equilibrium, calculated following Nemitz et al. (2000),

$$H(t) = \frac{161500}{T}e^{-10380/T}, \quad (3)$$

More details of the development of this diurnal variability scheme can be found in Zhu et al. (2015).

4.2 Evaluation with in situ NH_3 observations

We replace the standard GEOS-Chem livestock emissions, which are evenly distributed for each hour of the day (static), with this new diurnal variability of livestock emissions that peaks in the middle of the day (dynamic) (Figure 1). This also introduces daily variability of livestock emissions into the simulation, which is not considered in the standard GEOS-Chem model. As the standard GEOS-Chem anthropogenic emissions do not distinguish the livestock emissions sector (described in Section 2.1), we calculate the absolute NH_3 livestock emissions based on the fraction of livestock emissions in anthropogenic emissions in the 2008 NEI.

Significant improvements are found when we compare surface NH_3 concentrations to SEARCH observations after implementing the dynamic diurnal emissions (see Figure 2). The dynamic case (black) decreases the surface NH_3 concentration relative to the static case (red) by several ppb at night and increases concentrations slightly (up to 1 ppb) in the day. This reduces the model mean bias by up to 2.9 ppb at night.

4.3 Global distribution

To apply the dynamic emissions scheme globally, we implement a new global NH_3 anthropogenic emissions inventory Magnitude And Seasonality of AGricultural Emissions model (MASAGE_NH_3, Paulot et al. (2014)), which contains sector-specific emissions for different agriculture sources, such as livestock emissions (the standard GEOS-Chem NH_3 emissions do not clearly distinguish this sector). Comparisons between the emissions of MASAGE_NH_3 and GEOS-Chem standard inventories are in Paulot et al. (2014). Figure 3 shows the global distribution of surface NH_3 concentrations from the GEOS-Chem static and dynamic cases in April, July, and October of 2008. The third column shows the difference between the dynamic and the static cases. In general, the dynamic case decreases the monthly NH_3 surface concentration throughout the world with significant changes in Southeast China and India in all three months, which can be up to 17.1 ppb in China in October and 12.1 ppb in India in April. There are also large decreases in the Eastern US (up to 3.3 ppb) and southeastern of South America.

The modeled Representative Volume Mixing Ratio (RVMR) (Shephard et al., 2011) underestimates the observed RVMR from TES in the US and most places of the globe (Shephard et al., 2011; Zhu et al., 2013). In this study, we also compare the modeled RVMR from static and dynamic cases to the TES RVMR. We calculate modeled RVMR at the same time and locations of TES retrievals during 2006 through 2009. We average the RVMRs at the $2^\circ \times 2.5^\circ$ grid resolution for each month (April, July, and October). The static RVMR underestimates the TES RVMR throughout the globe in all three months except in India and Southeastern China in April. With the new diurnal variability scheme (dynamic case), the modeled RVMR increases in many places (e.g., Eastern China, Northern India, South America) and decreases in the Middle US and Northern Europe. The differences between the dynamic and static RVMR are from -1.5 ppb to 1.6 ppb. These changes generally reduce differences between modeled and observed RVMR, while the differences are enhanced in a few locations, such as Northern India in April. However, the magnitude of these changes is small compared to the differences (from -11.4 ppb to 3 ppb) between the static RVMR and TES RVMR. We are able to detect more obvious changes between the static and dynamic cases when focusing on a livestock source region (California) and a hotter day, during which the dynamic RVMR increases 3.4 ppb (Zhu et al., 2015). Stronger constraints on diurnal variability would be evident from potential future geostationary measurements (Zhu et al., 2015).

High biases of surface nitrate aerosol concentrations in GEOS-Chem are found in the US (e.g., Heald et al., 2012; Walker et al., 2012). Here we consider the impact of dynamic NH_3 livestock emissions on surface nitrate concentration in the US, as well as globally. Figure 4 presents the global distribution of surface nitrate concentration from the GEOS-Chem static and dynamic cases in April, July, and October of 2008. The dynamic case decreases the nitrate concentration significantly in Eastern China in all three months, which can be as large as 7 μg m^{-3} in October. There are also large decreases in the Eastern US which can be up to 2.7 μg m^{-3} in July. In October, there are large decreases in the dynamic case in comparison to static case in Northern India (up to 3.9 μg m^{-3}) and Europe (up to 2.4 μg m^{-3} in Poland).

Investigating the impacts of dynamic NH_3 livestock emissions on nitrogen deposition is also of interest. In Figure 5, we show the global distribution of total nitrogen deposition (wet deposition of NH_3, ammonium, HNO_3 and nitrate, and dry deposition of NH_3, ammonium, NO_2, PAN, N_2O_5, HNO_3 and nitrate) from GEOS-Chem static and dynamic cases in April, July, and October of 2008. The dynamic case decreases nitrogen deposition in most places in the world, yet increases it in several locations. The largest decrease of nitrogen deposition occurs in Northern India in April by up to 3.6 kg N/ha/month. The total amount of nitrogen deposition in India decreases by 8.6% in April. Decreases in nitrogen deposition in the dynamic case occur in Southeastern China in all three months, with the total amount of nitrogen deposition in China decreasing by 4.7% in April, 2.8% in July, 3.1% in October. The new diurnal variability scheme has more NH_3 from livestock emissions emitted in the daytime, when the boundary layer is thicker than nighttime. Typically, this lowers

deposition largely at night. However, it may also be conducive to more export of NH_3 in the atmosphere during the day. Thus, slight increases of nitrogen in the dynamic cases occur downwind of regions with large NH_3 sources in the base cases, such as increases in northeastern China owing to enhanced NH_3 export from Eastern China.

5 Bi-directional exchange of NH_3

5.1 Bi-directional flux calculation

The dry deposition scheme in the standard GEOS-Chem model is based on the resistance in series formulation of Wesely (1989), which only considers the unidirectional flux of NH_3 from the air to the surface. However, the air-surface exchange is known to actually be bi-directional. In this paper, we update the dry deposition of NH_3 to combine NH_3 dry deposition from the atmosphere and emission from vegetation. A simplified schematic of the updated air-surface exchange process of NH_3 is shown in Figure 6. More details of this bi-directional scheme can be found in Cooter et al. (2010) and Pleim et al. (2013). The total air-surface exchange flux, F_t, is calculated as a function of the gradient between the ambient NH_3 concentration in the first (surface) layer of the model and the canopy compensation point (Bash et al., 2013; Pleim et al., 2013),

$$F_t = \frac{C_c - C_a}{R_a + 0.5R_{inc}}, \tag{4}$$

where C_a is the ambient NH_3 concentration of the first atmospheric layer of the model, C_c is the canopy compensation point (which is set at one half of the in-canopy resistance, since NH_3 can come from either air or soil to the canopy, thus, splitting R_{inc} symmetrically is appropriate), R_a is the aerodynamic resistance, and R_{inc} is the in-canopy aerodynamic resistance. $C_a > C_c$ will result in deposition from air to surface, and $C_a < C_c$ will result in emission from surface to air. C_c is calculated as (Bash et al., 2013),

$$C_c = \frac{\frac{C_a}{R_a+0.5R_{inc}} + \frac{C_{st}}{R_b+R_{st}} + \frac{C_g}{0.5R_{inc}+R_{bg}+R_{soil}}}{(R_a+0.5R_{inc})^{-1} + (R_b+R_{st})^{-1} + (R_b+R_w)^{-1} + (0.5R_{inc}+R_{bg}+R_{soil})^{-1}}, \tag{5}$$

where R_b, R_{bg}, R_{st}, R_{soil} and R_w are the resistances at the quasi-laminar boundary layer of leaf surface, the quasi-laminar boundary layer of ground surface, the leaf stomatal, soil and cuticle respectively. R_a, R_b, R_{bg}, R_{st} and R_w are already defined and used in the standard GEOS-Chem deposition scheme. Here we define and calculate R_{soil} and R_{inc} following Pleim et al. (2013). C_{st} and C_g are the NH_3 concentrations in the leaf stomata and soil pores respectively. They are calculated as functions of temperature and NH_3 emission potential ($\Gamma_{st,g}$, dimensionless) in the leaf stomata and soil (Nemitz et al., 2000).

$$\Gamma = \frac{[NH_4^+]}{[H^+]}. \tag{6}$$

Γ_{st} is calculated as a function of land cover type, and the values of different land cover types are based on Zhang et al. (2010). Γ_g is calculated as a function of soil pH and NH_4^+ concentration

in the soil, $[NH_4^+]_{soil}$. Soil pH data is taken from ISRIC - World Soil Information with a 0.5° × 0.5° global resolution (http://www.isric.org/data/data-download). We model the $[NH_4^+]_{soil}$ as an ammonium pool in the soil, which is a function of fertilizer application rate, deposition, nitrification, soil moisture, and emission in bi-directional exchange. The calculation of $[NH_4^+]_{soil}$ is described in the next section.

To compare the deposition (downward) flux and emission (upward) flux of the bi-directional case to the base case, we define diagnostic variables for gross deposition flux F_{dep} and emission flux F_{emis} as follows (Bash et al., 2013),

$$F_{dep} = \frac{C_c - C_a}{R_a + 0.5R_{inc}}\Big|_{C_{st}=0, C_g=0}, \tag{7}$$

$$F_{emis} = \frac{C_c}{R_a + 0.5R_{inc}}\Big|_{C_a=0}, \tag{8}$$

where F_{dep} is calculated under the assumption that there is no NH_3 emission potential from the soil and canopy, and F_{emis} is calculated under the assumption that there is no NH_3 in the atmosphere. Thus, $F_{dep} + F_{emis} = F_t$.

5.2 Soil ammonium pool

Here we introduce a NH_4^+ pool to track the NH_3 and NH_4^+ in the atmosphere and in the soil. The inputs to the ammonium pool in the soil are NH_x (NH_3 and NH_4^+) deposition from the atmosphere, NH_3 emission from the soil, and N fertilizer application rate. The annual N fertilizer application rates are from Potter et al. (2010), which has chemical fertilizer (global total 70 Tg N yr^{-1}) with a 0.5° × 0.5° resolution for the year 2000. We assume that all forms of N fertilizers will convert to NH_4^+ rapidly after fertilizer application. This dataset is also used to develop the global soil nitric oxide emissions in GEOS-Chem in Hudman et al. (2012). We use the same treatment of annual total fertilization as Hudman et al. (2012) to derive daily fertilizer application rates by applying 75% of the annual total fertilization amount around the first day of the growing season (green-up day), distributed with a Gaussian distribution one month after. The other 25% is evenly distributed over the remaining time before the end of the growing season (brown-down day). The determination of green-up and brown-down days is based on the growing season dates derived from the MODIS Land Cover Dynamics product (MCD 12Q2) using the MODIS enhanced vegetation index (EVI) (Hudman et al., 2012).

Using the fertilizer inputs described above, in addition to inputs from deposition and outputs from emission, the time dependent soil NH_4^+ pool [mol L^{-1}] is calculated as

$$[NH_4^+]_{soil} = \frac{[NH_x]_{dep}}{d_s \theta N_A} + \frac{[N]_{fert}}{d_s \theta M_N} - \frac{[NH_3]_{bidiemit}}{d_s \theta N_A}, \tag{9}$$

where $[NH_x]_{dep}$ [molec cm^{-2}] is deposition from wet and dry deposition of NH_3 and NH_4^+, $[N]_{fert}$ [N g m^{-2}] is the NH_4^+ from fertilizer, $[NH_3]_{bidiemit}$ [molec cm^{-2}] is the gross NH_4^+ emitting from

the soil due to bi-directional exchange, M_N is the molar mass of nitrogen, d_s is the depth of the soil layer, taken to be 0.02 m, θ is the soil wetness [m^3 m^{-3}], and N_A is Avogadro's number. We then solve the mass balance equation for $[NH_x]_{dep}$ and $[N]_{fert}$,

$$\frac{d[\mathrm{NH}_x]_{dep}}{dt} = S_{dep} - \frac{[\mathrm{NH}_x]_{dep}}{\tau} - L_{dep}, \tag{10}$$

$$\frac{d[\mathrm{N}]_{fert}}{dt} = S_{fert} - \frac{[\mathrm{N}]_{fert}}{\tau}, \tag{11}$$

where τ is the decay time owing to nitrification rate of NH_4^+ in soil. We assume τ is 15 days, since almost all NH_4^+ will convert to NO_3^- within that timespan (Matson et al., 1998). S_{dep} is the deposition rate, S_{fert} is the fertilizer application rate, and L_{dep} is the deposition loss rate. We use the same assumption as Hudman et al. (2012) that only 60% of this deposited NH_x will enter the soil, while the rest of the NH_x deposition will runoff into waterways. Here we do not consider the production of NH_4^+ from NO_3^- in the nitrogen cycle from mineralization nor immobilization. The time scale of these processes can be years, which is much larger than the time scale of the NH_4^+ simulations considered here; Cooter et al. (2010) also found these processes were not needed to accurately simulate NH_3 over managed lands on similar time scales.

5.3 Adjoint of bi-directional exchange

To investigate the sensitivity of modeled NH_3 concentrations to the parameters in the bi-directional exchange model, and to facilitate future inverse modeling, we develop the adjoint of our updated NH_3 flux scheme. Here we consider two key parameters, soil pH and fertilizer application rate, since their values are highly approximate.

The adjoint sensitivity is defined as

$$\lambda_\sigma = \frac{\partial J(\mathrm{NH}_3)}{\partial \sigma}, \tag{12}$$

where $J(NH_3)$ is the total mass of ammonia at surface level in each grid box during 1 week. The unit of $J(NH_3)$ is kg/box. σ in this study is defined as the soil pH scaling factor (σ_{pH}) or fertilizer application rate scaling factor (σ_{fert_rate}). σ_{pH} is defined as $\frac{pH}{pH^0}$ and σ_{fert_rate} is defined as $\frac{fert\_rate}{fert\_rate^0}$. pH^0 and $fert\_rate^0$ are the initial estimate of soil pH from ISRIC and fertilizer application rates from Potter et al. (2010). λ_σ is the sensitivity of $J(NH_3)$ with respect to the bi-directional exchange model parameters σ.

5.4 Validating the adjoint of bi-directional exchange

We validate the accuracy of the adjoint model by comparing the sensitivity of NH_3 surface concentrations with respect to soil pH and fertilizer application rate calculated using the adjoint model with sensitivities calculated using the finite differences method. In order to make such comparisions efficiently throughout the model domain, horizontal transport is turned off for these tests (e.g.,

Henze et al., 2007). Figure 7 shows the comparison of sensitivities calculated by adjoint and finite difference. The cost function is evaluated once at the end of a one week simulation. The slope of a linear regression and square of correlation coefficient, R^2, are both close to unity, demonstrating the accuracy of adjoint of the bi-directional model.

6 Results and Discussion

For the US region, we use nested horizontal resolution (1/2 $^\circ\times$ 2/3°) simulations with the standard set of GEOS-Chem emission inventories. For the global simulation, we introduce a new bottom up emission inventory for NH_3 agriculture sources, MASAGE_NH3 (Paulot et al., 2014). The full description of the differences between the GESO-Chem standard NH_3 emission inventories and MASAGE_NH3 is in Paulot et al. (2014). We perform global simulation at a horizontal resolution of 2 $^\circ\times$ 2.5°. All simulations include the dynamic treatment of the diurnal variability of livestock emissions described in section 4.

6.1 US

We run the GEOS-Chem model for April, July, and October of 2008 with the updated diurnal variation of NH_3 livestock emissions and the bi-directional exchange mechanism. Figure 8 shows the NH_3 total gross emissions from GEOS-Chem with (BIDI) and without (BASE) the bi-directional air-surface exchange. The total gross emissions of BIDI case are the sum of primary emissions and upward fluxes from soil and vegetation. Bi-directional exchange generally increases gross emissions in most parts of the US in July (up to 0.43 Gg/month) and decreases gross emissions throughout the US in October (up to 0.29 Gg/month). Significant decreases occur in the Great Plains region in both April and October with a magnitude of up to 0.23 Gg/month in April and 0.29 Gg/month in October. Bi-directional exchange does not much alter the total modeled emissions in the US in July (increase by 5.2%) and October (decrease by 13.9%), but does lead to a decrease of 23.5% in April. With the ammonium soil pool, the model can preserve ammonia/ammonium in the soil rather than emitting it directly after fertilizer application. This is the main reason that gross emissions decrease in the Great Plains in April and October. In July, there is not as much fertilizer applied as in April. However, the bi-directional exchange between the air and surface can induce NH_3 to be re-emitted from the ammonium soil pool which reserve ammonium from previous deposition and fertilizer application.

The spatial distributions of surface NH_3 concentrations in GEOS-Chem are shown in Figure 9. In general, bi-directional exchange decreases monthly NH_3 surface concentrations in April (up to 1.8 ppb) and October (up to 2.1 ppb), and increases it in July (up to 2.8 ppb) throughout the US. There are peak decreases in NH_3 surface concentrations in the Great Plains in both April and October and increases in California in July. These changes of surface NH_3 concentration are consistent with the pattern of changes to NH_3 emissions in Figure 8.

6.1.1 Evaluation with NH_3

We evaluate the GEOS-Chem simulation with bi-directional exchange by comparing the model values to in situ observations from AMoN. Figure 10 shows the comparison of GEOS-Chem surface NH_3 concentrations in the BASE and BIDI cases with AMoN observations. Bi-directional exchange decreases the normalized mean bias (NMB) from -0.227 to -0.165 in July, and increases the NMB from -0.701 and -0.197 to -0.829 and 0.283 in April and October, respectively. The root mean square error (RMSE) decreases by 18.3% in July, and increases by 16.7% in April and 19.2% in October. R^2 values increase by 20.6% in July, and decrease by 37.6% in April and 49.1% in October. The slope slightly increases by 0.5% in July, and decreases by 53.5% and 37.5% in April and October, respectively. The changes in slopes can also be seen in Figure 9 as bi-directional exchange decreases the NH_3 monthly average concentration at AMoN sites in April and October while it increases the NH_3 monthly average concentrations in July. Modeled surface NH_3 concentrations are significantly lower than the AMoN observations in April and October by a factor of 2 - 5, which is not unreasonable given likely underestimates in primary emissions (Zhu et al., 2013; Nowak et al., 2012; Schiferl et al., 2014). Such large underestimation is not corrected by applying the NH_3 bi-directional exchange to the model. Other improvements in the model besides bi-directional exchange, such as updating primary NH_3 emissions, are also required for better estimating NH_3 surface concentrations.

6.1.2 Evaluation with aerosol nitrate

We also compare the simulated nitrate aerosol concentrations to the aerosol observations from IMPROVE. Figure 11 shows the simulated monthly average nitrate aerosol surface concentration from the GEOS-Chem BASE and BIDI cases in comparison to IMPROVE observations in 2008. GEOS-Chem overestimates nitrate in the BASE case in all three months. The overestimates in BASE cases can be 5 times larger in October. Bi-directional exchange generally decreases the nitrate concentrations in April, which makes the slope of the regression line decrease by 45.4%. However there are still large overestimates ($\sim$ a factor of 2 on average) in the Northeast US and large underestimates (up to 1.7 μg m^{-3}) in South California in the BIDI case in April. Bi-directional exchange slightly increases (less than 0.5 μg m^{-3}) nitrate in July and decreases (less than 0.4 μg m^{-3}) nitrate in October, which does not significantly impact the comparison of modeled nitrate with IMPROVE observations.

Overestimation of nitrate in GEOS-Chem is a long recognized problem (Park et al., 2004; Liao et al., 2007; Henze et al., 2009; Heald et al., 2012; Walker et al., 2012; Zhu et al., 2013). Heald et al. (2012) recommend that reducing the nitric acid to 75% would bring the magnitude of nitrate aerosol concentration into agreement with the IMPROVE observations. In our study, based on the comparison of BASE modeled nitrate concentration and IMPROVE observation, we perform sensitivity studies by reducing the nitric acid to 50% in July and to 20% in October at each timestep in

the GEOS-Chem model for both BASE and BIDI cases. Modeled nitrate concentrations reduce dramatically with this adjustment in July and October, but overestimates still exist in many places in the Eastern US. We also compare the modeled NH_3 surface concentrations in the sensitivity simulations with adjusted nitric acid concentrations to the AMoN observations, since reducing the nitric acid in the model may cause NH_3 to partition more to the gas phase, which could bring modeled NH_3 concentrations into better agreement with AMoN observations. However, no significant impacts are found in NH_3 concentrations at AMoN site locations with these nitric acid adjustments, consistent with earlier assessments that the model's nitrate formation is NH_3 limited throughout much of the US (Park et al., 2004). Overall, overestimation of model nitrate by a factor of 3 to 5 appears to be a model deficiency beyond the issue of NH_3 bi-directional exchange.

6.1.3 Comparison to inverse modeling

Inverse modeling estimates of uni-directional NH_3 emissions using TES observations lead to overestimates of ammonia concentration in comparison to surface observations from AMoN in July (Zhu et al., 2013), and emissions estimates in July are much higher than other top-down or bottom up studies (Paulot et al., 2014). It is thus of interest to evaluate whether bi-directional exchange of NH_3 would reduce this high bias. Although repeating the inverse modeling with TES NH_3 observations and bi-directional exchange is beyond the scope of this work, we can use the optimized emissions from Zhu et al. (2013) as the basis upon which bi-directional exchange is applied. Figure 12 shows the modeled NH_3 monthly average surface concentrations in comparison to the AMoN observations. The left column of Figure 12 is from the optimized NH_3 estimates from Zhu et al. (2013). In the right column, the modeled NH_3 monthly average concentrations are from GEOS-Chem with NH_3 bi-directional exchange using the optimized emissions from Zhu et al. (2013). The model with bi-directional exchange decreases the high bias in July: the NMB decreases by 80.4%; the RMSE decreases by 56.7%. The R^2 value increases by 43.3%. However, the model with bi-directional exchange now underestimates the NH_3 monthly average concentrations in April and October. The RMSE increases by 4.1% in April and 28.8% in October. The impacts of NH_3 concentration with respect to emissions in the model with bi-directional exchange are nonlinear. Using the optimized NH_3 emissions inventories from the TES NH_3 assimilation with the BASE model does not guarantee a better estimation of NH_3 surface concentrations with the BIDI model. Therefore, full coupling of inverse modeling with TES NH_3 observations and bi-directional exchange is necessary. Also, investigating the sensitivities of bi-directional model results to the NH_3 emissions, as well as other critical parameters, is important for improving the NH_3 concentration estimation.

6.2 Global modeling results

While bi-directional exchange of NH_3 has previously been implemented in regional models (e.g., Bash et al., 2013; Zhang et al., 2010; Wichink Kruit et al., 2012), with the GEOS-Chem model

we have the chance to evaluate NH_3 bi-directional exchange on global scales for the first time. The global distribution of NH_3 gross emissions in both BASE and BIDI cases, as well as their differences, are shown in Figure 13. Generally, bi-directional exchange decreases NH_3 emissions in the Northern Hemisphere, and increases NH_3 gross emissions in the Southern Hemisphere in April and October. Total NH_3 emissions in the Northern Hemisphere decrease by 22.6% in April and 7.8% in October. In July, bi-directional exchange increases NH_3 emissions in most places (7.1% globally), except China and India. As evident from the figure, the differences in many places throughout the globe are very slight. With positive and negative differences, the global mean and median of the changes are quite small (for example, the mean and median differences in July are -0.02 Gg/month and zero, respectively). However, there are areas where the differences deviate significantly from zero (for example the standard deviation of the difference in July is 3.76 Gg/month in China). We thus focus our discussion on the range of differences in particular regions that are evident from Figure 13.). Significant decreases in NH_3 emissions in the BIDI case occur in Southeastern China and Northern India in all three months. The magnitudes of the decreases can be up to 18.4 Gg/month in China and 16.5 Gg/month in India in July . Total NH_3 emissions in China decrease by 43.6% in April, 31.4% in July, and 24.7% in October. Total NH_3 emissions in India decrease by 28.8% in April, 22.8% in July, and 7.2% in October. There are also large decreases of total NH_3 emissions in the US, Mexico and Europe in April of up to 6.5 Gg/month.

The changes of NH_3 gross emissions between BASE and BIDI cases can be seen more directly from the comparison of fertilizers emissions in the BASE case with those in the BIDI case. In Figure 14, we show the global distribution of NH_3 fertilizer emissions in the BASE and BIDI cases. In BIDI case, the fertilizer emissions are the upward fluxes from soil and vegetation from bi-directional exchange. The third column is the NH_3 emissions from all other sources except fertilizers in April, July, and October of 2008. In the BASE case, fertilizers emissions have peak values in Eastern China and Middle East Asia and much smaller values elsewhere. Fertilizers emissions in the BIDI case increase in many places where there are no or near zero values in the BASE case. In the BIDI case, the fertilizer emissions distribution is much more homogeneous. As we described in Section 6.1, fertilizer emissions are lower in the BIDI case under cool spring and fall time conditions due to the temperature effects on NH_3 emissions and storage in the soil ammonium pool. The deposition and re-emission processes in bi-directional exchange model thus extend the effect of NH_3 emissions from fertilizers. There are obvious trends that fertilizer emissions in the Northern Hemisphere are larger than those in the Southern Hemisphere in April and July, and fertilizer emissions in the Southern Hemisphere are larger than those in the Northern Hemisphere in October. The global amount of NH_3 fertilizer emissions is 27.8% of total emissions from all sources in the BASE case and 12.8% in the BIDI case in April. Figure 15 shows the percentage of emissions from fertilizers in BIDI case in the global simulations. BIDI fertilizers contribute more to gross emissions in July than in other

months in the Northern Hemisphere, which again demonstrates the delayed effect of fertilizer NH_3 (mostly applied in the springtime) in the BIDI model.

Figure 16 shows the global distribution of NH_3 monthly surface concentrations in the BASE and BIDI cases and their differences in April, July and October. Although bi-directional exchange changes NH_3 concentrations slightly throughout the globe (mean and median values of the changes are all nearly zero in all three months), significant changes still exist in many places. In general, bi-directional exchange increases NH_3 concentrations in July by up to 3.9 ppb. It decreases NH_3 concentrations in the Northern Hemisphere (up to 27.6 ppb) and increases NH_3 concentrations in the Southern Hemisphere (up to 4.2 ppb) in April and October. Significant decreases of NH_3 concentrations occur in China in all three months with up to 20.6 ppb in April, 12.8 ppb in July, and 15.7 ppb in October. Paulot et al. (2014) indicated the MASAGE NH_3 emissions, which we use in this study, were higher than the bottom-up NH_3 emissions from Huang et al. (2012) in China in April and July, and similar to the emissions from Streets et al. (2003) in April, July, and October. Overestimation of NH_3 surface concentrations in GEOS-Chem in China are found in Wang et al. (2013) when using NH_3 emissions from Streets et al. (2003), leading to an overestimation of nitrate aerosol concentrations in China. Observations from the Infrared Atmospheric Sounding Interferometer (IASI) remote sensing instrument have discrepancies over China with NH_3 concentrations in GEOS-Chem (Kharol et al., 2013; Clarisse et al., 2009) that may in part be improved by the impacts of bi-directional exchange. However, observations from TES show NH_3 concentrations in GEOS-Chem (with NH_3 emissions from Streets et al. (2003)) are underestimated in many places of the globe including China (Shephard et al., 2011). We must note that the lower NH_3 concentrations presented here are daily averages, while IASI and TES data are for a particular hour of the day. The changes in the emissions profile may reduce the model underestimate against the satellite observations while decreasing the mean NH_3 concentrations. However, the ability of remote sensing instruments on satellites in low-earth orbits (LEO) to observe the impact of bidirectional exchange on NH_3 concentrations is limited compared to observations from potential future geostationary measurements (Zhu et al., 2015).

6.3 Wet deposition evaluation (Global and US)

We compare the model NH_4^+ wet deposition to in situ observations in several regions of the world using NTN for the continental US, CAPMoN for Canada, EMEP for Europe, and EANET for East Asia, see Figure 17. For the model NH_4^+ wet deposition, we also include the model NH_3 wet deposition since NH_4^+ wet deposition from in situ observations includes precipitated NH_3. Since there are biases in the modeled precipitation, we scale the model wet deposition by multiplying the modeled deposition by the ratio of the observed to modeled precipitation, $Flux_{model} * (\frac{P_{obs}}{P_{model}})^{0.6}$, following the correction method in Paulot et al. (2014). We only include observations that have $0.25 < \frac{P_{obs}}{P_{sim}} < 4$ to limit the effect of this correction (Paulot et al., 2014), and we also exclude ob-

servations which are beyond three times the standard deviation of observed NH_4^+ wet deposition to avoid outliers.

In general, the GEOS-Chem model underestimates NH_4^+ wet deposition throughout the world in the BASE case. Large increases in NH_4^+ wet deposition in the BIDI cases are found in the US, Canada, and Europe in July (up to 6.31 kg ha^{-1} yr^{-1}). The slopes of the regression line when compared to observations increase by 37.9% in US, 54.9% in Canada, and 17.7% in Europe in the BIDI cases in July, all becoming closer to unity. However, the bi-directional exchange increases the RMSE by 64.3% in the US, 37.2% in Canada, and 36.0% in Europe.

Bi-directional exchange does not impact the NH_4^+ wet deposition much in April and October. It decreases NH_4^+ wet deposition slightly (up to 3.77 kg ha^{-1} yr^{-1} in Europe) at most of the observation locations in the US, Canada, and Europe in April. The slopes decrease by 14.3% in the US, 6.8% in Canada, and 12.3% in Europe. Bi-directional exchange decreases the NMB by 46.4% in the US, 37.6% in Europe in April, but increases the NMB by 28.3% in Canada, and 11.6% in East Asia. In October, bi-directional exchange increases NH_4^+ wet deposition slightly at most of the observation locations (up to 3.85 kg ha^{-1} yr^{-1}). The changes in RMSE between BASE and BIDI cases are small, less than 10%.

The overall differences of NH_4^+ wet deposition between the BASE and BIDI cases are generally small (from -4.95 to 6.31 kg ha^{-1} yr^{-1}), even when the differences in NH_3 emissions are substantial. For example, NH_3 emissions differences between the BASE and BIDI range from -61.2 to 1.16 kg ha^{-1} yr^{-1} in China in April with bi-directional exchange, but changes in NH_4^+ wet deposition are not very large (from -4.95 to 2.52 kg ha^{-1} yr^{-1}). While implementing NH_3 bi-directional exchange leads to improvements in some regions and seasons, it does not uniformly reduce error in model estimation of NH_4^+ wet deposition.

6.4 Adjoint sensitivity analysis

6.4.1 Global adjoint sensitivities

In section 5.3, we demonstrated the accuracy of the sensitivities calculated using the adjoint of the GEOS-Chem bi-directional model. In this section, we present the adjoint sensitivities of NH_3 surface concentrations with respect to the important parameters in the bi-directional model. Figure 18 shows the adjoint sensitivities of NH_3 surface concentration with respect to the scaling factors for the soil pH (left) and for the fertilizer application rate (right) in April, July, and October, 2008. The sensitivities with respect to both parameters are always positive throughout the globe. Sensitivities of NH_3 to fertilizer application rate are positive as excess fertilizer application will increase the NH_3 soil emission potential. Sensitivities of NH_3 to soil pH are also positive as low H^+ concentrations in soil (high soil pH) increases dissociation of NH_4^+ to NH_3, thereby increasing the potential for volatilization of NH_3.

The relationship between NH_3 concentration and soil pH is stronger during the growing season since more ammonium is in the soil pool. Slight changes in pH may have large impacts on the amount of NH_3 emitted from soil and further induce large differences in NH_3 surface concentrations. As we can see in the left column of Figure 18, the sensitivities of NH_3 surface concentrations with respect to soil pH scaling factors are larger in the Northern Hemisphere than those in the Southern Hemisphere in April and July, and less in the Northern Hemisphere than those in the Southern Hemisphere in October, since the growing seasons are in April in the Northern Hemisphere and in October in the Southern Hemisphere. Large sensitivities in July in the Northern Hemisphere are due to ammonium in the soil pool accumulated from CAFO emissions via deposition. However, some caution is warranted in interpreting the seasonality of these sensitivities, as our model does not include any seasonal variations in soil pH. Seasonal variability of soil pH is driven by fertilizer rate, timing of fertilizer application, root and bacterial activity, soil moisture, organic matter, and salt levels (Murdock and Call, 2006). Soil pH is observed to be highest at or near mid-winter and lowest at late summer (Slattery and Ronnfeldt, 1992). Variation of soil pH can be more than one unit from spring to fall (Angima, 2010), thus the uncertainty in the constant annual soil pH used here could be about 20% owing to neglecting seasonality.

The relationship between NH_3 concentration and fertilizer application rate is also seasonally dependent. The seasonal trends of sensitivities of NH_3 to fertilizer application rate are similar to sensitivities of NH_3 to soil pH. Larger sensitivities appear in places with lower fertilizer application rates than those with plenty of fertilizer. For example, the largest fertilizer application rates appear in Southeast China, Northwest Europe and Northern India in April, and sensitivities are nearly zero in each of these locations. That the magnitude of the fertilizer application rates itself is an important factor in determining the sensitivities of NH_3 concentration to the fertilizer application rate is indicative of the nonlinear relationship introduced by treatment of bi-directional exchange.

Through investigating the sensitivities of NH_3 surface concentration to the soil pH and the fertilizer application rate, we know that NH_3 surface concentrations are very sensitive to these parameters in many places of globe. We also find that NH_3 surface concentrations are more sensitive to soil pH than fertilizer application rate in general. In addition to the adjoint sensitivity analysis of NH_3 concentrations to the soil pH and the fertilizer application rate, it is also interesting to know the ranking of sensitivities of NH_3 concentrations with respect to other parameters, such as NH_3 concentrations at compensation points (C_c, C_{st}, C_g), NH_3 emission potentials (Γ_g, Γ_{st}), and resistances (R_a, R_{inc}, R_{soil}, R_g, R_{st}, R_{bg}, R_w). Knowledge of the sensitivity of NH_3 concentrations with respect to these parameters may help improve the model estimation of the spatial and temporal distributions as well as the magnitudes of NH_3 concentrations.

6.4.2 Comparison to in situ NH_3 with adjusted BIDI parameters

Based on the adjoint sensitivity analysis we have shown above and forward sensitivity analysis for all the parameters mentioned above (results not shown), we know that soil pH is one of the most critical parameters in the GEOS-Chem bi-directional exchange model. It is interesting to explore to what extent biases in the modeled NH_3 concentrations may be explained by uncertainties in the parameters of the bi-directional model, rather than e.g., revising livestock NH_3 emissions. To test this, we increase the soil pH value by a factor of 1.1, since uncertainties of seasonal soil pH are about 20%. As expected, the NH_3 surface concentrations generally increase over the globe (e.g., up to 3.4 ppb in April). Large increases occur in places with large sensitivities to soil pH (Figure 18, upper left). NH_3 concentrations are underestimated in the model in comparison to the AMoN observations in the US. They are also underestimated in many parts of globe in comparison to TES observations (Shephard et al., 2011). With this adjustment to soil pH, the discrepancy between TES observations and the model in upper levels of the boundary layer may potentially be reduced in regions where GEOS-Chem NH_3 is underestimated before the growing seasons and overestimated after the growing seasons. Slight increases in NH_3 surface concentrations are found throughout the US as NH_3 is not very sensitive to soil pH in the US (see Figure 18). Thus, this adjustment does not improve the comparison to AMoN observations in the US.

In this study, we did not consider the adjustment of soil pH in agricultural areas by the farmers who limit the soil pH in a certain range to improve crop yield (Haynes and Naidu, 1998). However, no significant changes in the modeled surface NH_3 concentrations occur with bi-directional exchange when we limit the soil pH in the agricultural areas between 5.5 and 6.5 (generally less than 1 ppb over the globe, up to 3.4 ppb in India), since sensitivities are not very strong in the agricultural areas (see left column of Figure 18).

Small differences between bi-directional and unidirectional fluxes in the US are also indicated in Dennis et al. (2013), wherein sensitivity tests were performed varying the soil emission potential (Γ_g, a parameter which includes both soil pH and fertilizer application rate) in CMAQ. It was found that the impact on total N deposition at continental scales was generally small ($< 5\%$), with very few ($< 10\%$) grid cells having differences up to 20%.

From Zhu et al. (2013), we know that the underestimation of NH_3 emissions in the unidirectional model can be as much as a factor of 9 in the US. We also notice that NH_3 may not change much when fertilizer emissions increase a lot in regions such as Midwest US and Northern Australia (see Figure 14 and Figure 16). Thus, low emissions from other sources, such as livestock, may be a big part of the reason for underestimating NH_3 concentrations in the bi-directional exchange model. To better understand this, we also test increasing NH_3 livestock emissions by a factor of 8 in April and 3 in October as NH_3 concentrations are generally underestimated by around 8 and 3 times (Figure 10) compare to AMoN observations in April and October, respectively. These adjustments bring the NH_3 concentrations into a much better agreement with the magnitude of AMoN observations, see

Figure 19. However, uniformly increasing the livestock emissions does not well represent the NH_3 spatial distribution with the AMoN observations (correlations of model and observation are very low). Overall, treatment of bi-directional exchange can improve our understanding of NH_3 emissions from fertilizers, but this alone may not improve estimation of NH_3 concentrations, NH_4^+ wet depositions, and nitrate aerosol concentrations. Additional work including bi-directional exchange in NH_3 inverse modeling is needed, as large underestimates in NH_3 primary sources exist in the model and simply applying the scheme to optimized emissions from inverse modeling can not well capture the spatial variability of NH_3 concentrations that are the responses of both bi-directional exchange processes and emissions.

6.4.3 Spot sensitivity analysis

Here we investigate to what extent bi-directional exchange increases the NH_3 lifetime, which is a critical issue for controlling nitrogen deposition and $PM_{2.5}$ formation. Through the adjoint method, we are able to assess source contributions to model estimates in particular response regions (e.g., Lee et al., 2014). In Figure 20, we show the adjoint sensitivity of NH_3 surface concentration at a single location [88°W, 40°N] with respect to the NH_3 anthropogenic emissions at all grid cells in April, 2008. In the BASE case (left panel), the NH_3 surface concentration is most sensitive to the emissions from the same grid cell, and is less sensitive to the emissions from surrounding grid cells. With the bi-directional exchange (right panel), the NH_3 concentration is sensitive to the emissions from a much wider range, which extends all the way to Canada. Some of the sensitivities are very strong even though they are a long distance away from the location of the NH_3 concentration under consideration. The deposition and re-emission processes in the bi-directional exchange extends the spatial range of influence of NH_3 emissions and, in effect, the NH_3 lifetime. Thus, modeled NH_3 concentrations in Illinois can be impacted by the emissions from Kansas or even from Canada.

7 Conclusions

In this study, we have considered a more detailed, process-level treatment of NH_3 sources in a global chemical transport model (GEOS-Chem) and evaluated the model behavior in terms of biases in estimated NH_3, nitrate, and NH_4^+ wet deposition, and the factors driving these processes in the model. First, we update the diurnal variability of NH_3 livestock emissions. In general, by implementing this diurnal variability scheme, the global NH_3 concentrations, nitrate aerosol concentrations, and nitrogen deposition all decrease. The largest decreases always occur in Southeastern China and Northern India. More NH_3 from livestock emitted in the daytime largely decreases the NH_3 surface concentrations in the night and increases concentrations during the day, which is more conducive to export of NH_3.

We have also developed bi-directional exchange of NH_3 and its adjoint in the GEOS-Chem model. Bi-directional exchange generally increases NH_3 gross emissions in most parts of the US and most places around the globe in July, except China and India. These are mainly due to the NH_3 re-emissions from the ammonium soil pool that accumulates ammonium from previous months. Bi-directional exchange generally decreases NH_3 gross emissions in the US in April and October. On a global scale, bi-directional exchange decreases NH_3 gross emissions in the Northern Hemisphere in April and October, and increases NH_3 gross emissions in the Southern Hemisphere. During the growing seasons, the ammonium soil pool preserves ammonia/ammonium in the soil rather than emitting it directly after fertilizer application.

Bi-directional exchange increases monthly NH_3 surface concentrations throughout the world in July, which improves comparison to the AMoN observations in the US. It decreases NH_3 surface concentrations in the Northern Hemisphere and increases NH_3 concentrations in the Southern Hemisphere in April and October. Bi-directional exchange does not have a large impact on model biases in nitrate aerosol, which are likely owing to overestimated nitric acid concentration (Heald et al., 2012). However, with the deposition and re-emission of NH_3 inherent in bi-directional exchange, NH_3 can be impacted by sources from a much greater distance, which is a critical issue when considering strategies for controlling nitrogen deposition and $PM_{2.5}$ formation.

Bi-directional exchange largely increases NH_4^+ wet deposition in the US, Canada, and Europe in July, but slightly decreases NH_4^+ wet deposition in April and has little impact in October. The overall differences of NH_4^+ wet deposition between the BASE and BIDI cases are generally small, even when the differences in NH_3 fertilizer emissions are large. While observations of wet deposition have been used to constrain NH_3 sources in previous works (Gilliland et al., 2003, 2006; Zhang et al., 2012; Paulot et al., 2014), this dataset does not appear sufficient to provide constraints on model treatment of bi-directional exchange. Moreover, as the in situ measurements used here are limited in space and time, the comparisons between model and measurements only represents the ability of bi-directional parameterization at these specific spatial (100′s of km) and temporal (monthly) scales; more pronounced impacts may occur at finer scales.

Using the adjoint of bi-directional exchange, we investigate the spatial and seasonal dependency of NH_3 surface concentrations in the GEOS-Chem model on the soil pH and fertilizer application rate, which are themselves uncertain. Soil pH is known to be seasonally variable. Updating the soil pH with seasonal variability would impact the results of bi-directional exchange across wide regions of globe. However, updating the soil pH with seasonal variability does not seem sufficient to improve comparison with in situ observations in the US, as primary sources are likely underestimated by a factor of 3 or more. Further, uniformly increasing the emissions from primary sources degrades the spatial variability of simulated NH_3.

Overall, bi-directional exchange largely extends the lifetime of NH_3 in the atmosphere via deposition and re-emission processes. This model provides a better fundamental description of NH_3

emissions from fertilizers. However, implementing bi-directional exchange does not uniformly improve estimation of NH_3 concentrations, NH_4^+ wet deposition, and nitrate aerosol concentrations. Domain-wide adjustments to soil pH or livestock emissions do not improve the model comparison to the full suite of measurements from different platforms, locations and seasons considered here. Thus, incorporating bi-directional exchange in an inverse model is required in future work to correct the low biases in NH_3 primary sources without over adjusting these sources to account for model error from neglecting bi-directional exchange processes. Measurements from recent (Shephard and Cady-Pereira, 2015) or future (Zhu et al., 2015) remote sensing platforms will be of value for such endeavors.

Acknowledgements. This work is supported by NASA grants NNX09AN77G and NNX10AG63G and EPA STAR award RD834559. While this manuscript has been reviewed by the Environmental Protection Agency and approved for publication, it may not reflect official agency views or policies.

References

Angima, S.: Measuring Soil pH, Oregon State University Small Farms Program, 2010.

Bash, J., Walker, J., Katul, G., Jones, M., Nemitz, E., and Robarge, W.: Estimation of in-canopy ammonia sources and sinks in a fertilized Zea Mays field, Environ. Sci. Technol, 44, 1683–1689, 2010.

Bash, J. O., Cooter, E. J., Dennis, R. L., Walker, J. T., and Pleim, J. E.: Evaluation of a regional air-quality model with bidirectional NH3 exchange coupled to an agroecosystem model, Biogeosciences, 10, 1635–1645, doi:10.5194/bg-10-1635-2013, 2013.

Bey, I., Jacob, D. J., Yantosca, R. M., Logan, J. A., Field, B. D., Fiore, A. M., Li, Q. B., Liu, H. G. Y., Mickley, L. J., and Schultz, M. G.: Global modeling of tropospheric chemistry with assimilated meteorology: Model description and evaluation, J. Geophys. Res.-Atmos., 106, 23 073–23 095, 2001.

Bouwman, A. F., Lee, D. S., Asman, W. A. H., Dentener, F. J., VanderHoek, K. W., and Olivier, J. G. J.: A global high-resolution emission inventory for ammonia, Global Biogeochem. Cycles, 11, 561–587, 1997.

Ciais, P., Sabine, C., Bala, G., Bopp, L., Brovkin, V., Canadell, J., Chhabra, A., DeFries, R., Galloway, J., Heimann, M., Jones, C., Quéré, C. L., Myneni, R., Piao, S., and Thornton, P.: Carbon and Other Biogeochemical Cycles, in Climate Change 2013, The Physical Science Basis. Contribution of Working Group I to the Fifth Assessment Report, pp. 465–570, 2013.

Clarisse, L., Clerbaux, C., Dentener, F., Hurtmans, D., and Coheur, P. F.: Global ammonia distribution derived from infrared satellite observations, Nature Geoscience, 2, 479–483, doi:Doi 10.1038/Ngeo551, 2009.

Cooter, E. J., Bash, J. O., Walker, J. T., Jones, M., and Robarge, W.: Estimation of NH_3 bi-directional flux from managed agricultural soils, Atmospheric Environment, 44, 2107 – 2115, doi:http://dx.doi.org/10.1016/j.atmosenv.2010.02.044, 2010.

Crouse, D. L., Peters, P. A., van Donkelaar, A., Goldberg, M. S., Villeneuve, P. J., Brion, O., Khan, S., Atari, D. O., Jerrett, M., Pope, C. A., Brauer, M., Brook, J. R., Martin, R. V., Stieb, D., and Burnett, R. T.: Risk of Non accidental and Cardiovascular Mortality in Relation to Long-term Exposure to Low Concentrations of Fine Particulate Matter: A Canadian National-Level Cohort Study, Environ. Health Perspect., 120, 708–714, doi:10.1289/ehp.1104049, 2012.

Dennis, R., Schwede, D., Bash, J., Pleim, J., Walker, J., and Foley, K.: Sensitivity of continental United States atmospheric budgets of oxidized and reduced nitrogen to dry deposition parametrizations, Phil. Trans. R. Soc. B, 368, doi:10.1098/rstb.2013.0124, 2013.

Elbern, H., Schmidt, H., and Ebel, A.: Variational data assimilation for tropospheric chemistry modeling, J. Geophys. Res.-Atmos., 102, 15 967–15 985, 1997.

Elbern, H., Schmidt, H., Talagrand, O., and Ebel, A.: 4D-varational data assimilation with an adjoint air quality model for emission analysis, Environ. Modell. Softw., 15, 539–548, 2000.

Fisher, M. and Lary, D. J.: Lagrangian four-dimensional variational data assimilation of chemical species, Q. J. R. Meteorol. Soc., 121, 1681–1704, 1995.

Galloway, J. N., Townsend, A. R., Erisman, J. W., Bekunda, M., Cai, Z. C., Freney, J. R., Martinelli, L. A., Seitzinger, S. P., and Sutton, M. A.: Transformation of the nitrogen cycle: Recent trends, questions, and potential solutions, Science, 320, 889–892, doi:10.1126/Science.1136674, 2008.

Gilliland, A. B., Dennis, R. L., Roselle, S. J., and Pierce, T. E.: Seasonal NH_3 emission estimates for the eastern United States based on ammonium wet concentrations and an inverse modeling method, J. Geophys. Res.-Atmos., 108, 4477, doi:10.1029/2002JD003063, 2003.

Gilliland, A. B., Appel, K. W., Pinder, R. W., and Dennis, R. L.: Seasonal NH_3 emissions for the continental United States: Inverse model estimation and evaluation, Atmos. Environ., 40, 4986–4998, 2006.

Haynes, R. and Naidu, R.: Influence of lime, fertilizer and manure applications on soil organic matter content and soil physical conditions: a review, Nutrient Cycling in Agroecosystems, 51, 123–137, doi:10.1023/A:1009738307837, 1998.

Heald, C. L., Collett Jr., J. L., Lee, T., Benedict, K. B., Schwandner, F. M., Li, Y., Clarisse, L., Hurtmans, D. R., Van Damme, M., Clerbaux, C., Coheur, P.-F., Philip, S., Martin, R. V., and Pye, H. O. T.: Atmospheric ammonia and particulate inorganic nitrogen over the United States, Atmos. Chem. Phys., 12, 10 295–10 312, doi:10.5194/acp-12-10295-2012, 2012.

Henze, D. K., Hakami, A., and Seinfeld, J. H.: Development of the adjoint of GEOS-Chem, Atmos. Chem. Phys., 7, 2413–2433, 2007.

Henze, D. K., Seinfeld, J. H., and Shindell, D.: Inverse modeling and mapping U.S. air quality influences of inorganic $PM_{2.5}$ precursor emissions using the adjoint of GEOS-Chem, Atmos. Chem. Phys., 9, 5877–5903, 2009.

Huang, X., Song, Y., Li, M., Li, J., Huo, Q., Cai, X., Zhu, T., Hu, M., and Zhang, H.: A high-resolution ammonia emission inventory in China, Global Biogeochem. Cycles, 26, doi:10.1029/2011GB004161, 2012.

Hudman, R. C., Moore, N. E., Mebust, A. K., Martin, R. V., Russell, A. R., Valin, L. C., and Cohen, R. C.: Steps towards a mechanistic model of global soil nitric oxide emissions: implementation and space based-constraints, Atmos. Chem. Phys., 12, 7779–7795, doi:10.5194/acp-12-7779-2012, 2012.

Kharol, S. K., Martin, R. V., Philip, S., Vogel, S., Henze, D. K., Chen, D., Wang, Y., Zhang, Q., and Heald, C. L.: Persistent sensitivity of Asian aerosol to emissions of nitrogen oxides, Geophys. Res. Lett., doi:10.1002/grl.50234, 2013.

Kopacz, M., Jacob, D., Fisher, J., Logan, J., Zhang, L., Megretskaia, I., Yantosca, R., Singh, K., Henze, D., Burrows, J., Buchwitz, M., Khlystova, I., McMillan, W., Gille, J., Edwards, D., Eldering, A., Thouret, V., and Nedelec, P.: Global estimates of CO sources with high resolution by adjoint inversion of multiple satellite datasets (MOPITT, AIRS, SCIAMACHY, TES), Atmos. Chem. Phys., 10, 855–876, 2010.

Lamarque, J.-F., Kyle, G., Meinshausen, M., Riahi, K., Smith, S., van Vuuren, D., Conley, A., and Vitt, F.: Global and regional evolution of short-lived radiatively-active gases and aerosols in the Representative Concentration Pathways, IClimatic Change, 109, 191?212, doi:10.1007/s10584-011-0155-0, 2011.

Langridge, J. M., Lack, D. A., Brock, C. A., Bahreini, R., Middlebrook, A. M., Neuman, J. A., Nowak, J. B., Perring, A. E., Schwarz, J. P., Spackman, J. R., Holloway, J. S., Pollack, I. B., Ryerson, T. B., Roberts, J. M., Warneke, C., de Gouw, J., Trainer, M. K., and Murphy, D. M.: Evolution of aerosol properties impacting visibility and direct climate forcing in an ammonia-rich urban environment, J. Geophys. Res., 117, D00V11, doi:10.1029/2011JD017116, 2012.

Lee, H.-M., Henze, D., Alexander, B., and Murray, L.: Investigating the sensitivity of surface-level nitrate seasonality in Antarctica to primary sources using a global model, Atmospheric Environment, doi:10.1016/j.atmosenv.2014.03.003, 2014.

Liao, H., Henze, D. K., Seinfeld, J. H., Wu, S., and Mickley, L. J.: Biogenic secondary organic aerosol over the United States: Comparison of climatological simulations with observations, J. Geophys. Res.-Atmos., 112, D06201, doi:10.1029/2006JD007813, 2007.

Liu, H. Y., Jacob, D. J., Bey, I., and Yantosca, R. M.: Constraints from Pb-210 and Be-7 on wet deposition and transport in a global three-dimensional chemical tracer model driven by assimilated meteorological fields, J. Geophys. Res., 106, 12 109–12 128, 2001.

Liu, X., Zhang, Y., Han, W., Tang, A., Shen, J., Cui, Z., Vitousek, P., Erisman, J. W., Goulding, K., Christie, P., Fangmeier, A., and Zhang, F.: Enhanced nitrogen deposition over China, Nature, 494, 459–462, doi:10.1038/nature11917, 2013.

Malm, W. C., Schichtel, B. A., Pitchford, M. L., Ashbaugh, L. L., and Eldred, R. A.: Spatial and monthly trends in speciated fine particle concentration in the United States, J. Geophys. Res.-Atmos., 109, D03306, doi:10.1029/2003jd003739, 2004.

Martien, P. T. and Harley, R. A.: Adjoint sensitivity analysis for a three-dimensional photochemical model: Application to Southern California, Environ. Sci. Technol., 40, 4200–4210, 2006.

Matson, P. A., Naylor, R. L., and Ortiz-Monasterio, I.: Integration of environmental, agronomic, and economic aspects of fertilizer management, Science, 280, 112–115, 1998.

Murdock, L. and Call, D.: Managing Seasonal Fluctuations of Soil Tests, University of Kentucky Cooperative Extension, 2006.

Nemitz, E., Sutton, M. A., Schjoerring, J. K., Husted, S., and Wyers, G. P.: Resistance modelling of ammonia exchange above oilseed rape, Agricultural and Forest Meteorology, 105, 405–425, 2000.

Nemitz, E., Milford, C., and Sutton, M. A.: A two-layer canopy compensation point model for describing bi-directional biosphere-atmosphere exchange of ammonia, Q. J. Roy. Meteor. Soc., 127, 815–833, 2001.

Nowak, J. B., Neuman, J. A., Bahreini, R., Middlebrook, A. M., Holloway, J. S., McKeen, S. A., Parrish, D. D., Ryerson, T. B., and Trainer, M.: Ammonia sources in the California South Coast Air Basin and their impact on ammonium nitrate formation, Geophys. Res. Lett., 39, L07804, doi:10.1029/2012GL051197, 2012.

Park, R. J., Jacob, D., Field, B. D., Yantosca, R., and Chin, M.: Natural and transboundary pollution influences on sulfate-nitrate-ammonium aerosols in the United States: Implications for policy, J. Geophys. Res.-Atmos., 109, D15204, doi:10.1029/2003JD004473, 2004.

Paulot, F., Jacob, D. J., Pinder, R. W., Bash, J. O., Travis, K., and Henze, D. K.: Ammonia emissions in the United States, European Union, and China derived by high-resolution inversion of ammonium wet deposition data: Interpretation with a new agricultural emissions inventory (MASAGE_NH3), J. Geophys. Res. Atmos., 119, 4343–4364, doi:10.1002/2013JD021130, 2014.

Pinder, R. W., Adams, P. J., Pandis, S. N., and Gilliland, A. B.: Temporally resolved ammonia emission inventories: Current estimates, evaluation tools, and measurement needs, J. Geophys. Res. Atmos., 111, D16310, doi:10.1029/2005JD006603, 2006.

Pinder, R. W., Walker, J. T., Bash, J. O., Cady-Pereira, K. E., Henze, D. K., Luo, M., Osterman, G. B., and Shephard, M. W.: Quantifying spatial and temporal variability in atmospheric ammonia with in situ and space-based observations, Geophys. Res. Lett., 38, doi:Doi 10.1029/2010GL046146, 2011.

Pleim, J. E., Bash, J. O., Walker, J. T., and Cooter, E. J.: Development and evaluation of an ammonia bidirectional flux parameterization for air quality models, J. Geophys. Res. Atmos., 118, doi:10.1002/jgrd.50262, 2013.

Pope, C. A., Ezzati, M., and Dockery, D. W.: Fine-particulate air pollution and life expectancy in the United States, N. Engl. J. Med., 360(4), 376?386, 2009.

Potter, P., Ramankutty, N., Bennett, E. M., and Donner, S. D.: Characterizing the spatial patterns of global fertilizer application and manure production, Earth Interact., 14, 1–22, 2010.

Puchalski, M. A., Sather, M. E., Walker, J. T., Lehmann, C. M., Gay, D. A., Mathew, J., and Robarge, W. P.: Passive ammonia monitoring in the United States: comparing three different sampling devices, J. Environ. Monit., 13, 3156–3167, 2011.

Reiss, R., Anderson, E. L., Cross, C. E., Hidy, G., Hoel, D., McClellan, R., and Moolgavkar, S.: Evidence of health impacts of sulfate- and nitrate-containing particles in ambient air, Inhal Toxicol, 19, 419–449, doi:10.1080/08958370601174941, 2007.

Schiferl, L. D., Heald, C. L., Nowak, J. B., Holloway, J. S., Neuman, J. A., Bahreini, R., Pollack, I. B., Ryerson, T. B., Wiedinmyer, C., and Murphy, J. G.: An investigation of ammonia and inorganic particulate matter in California during the CalNex campaign, J. Geophys. Res. Atmos., 119, 1883–1902, doi:10.1002/2013JD020765, 2014.

Shephard, M. W. and Cady-Pereira, K. E.: Cross-track Infrared Sounder (CrIS) satellite observations of tropospheric ammonia, Atmos. Meas. Tech., 8, 1323–1336, doi:10.5194/amt-8-1323-2015, 2015.

Shephard, M. W., Cady-Pereira, K. E., Luo, M., Henze, D. K., Pinder, R. W., Walker, J. T., Rinsland, C. P., Bash, J. O., Zhu, L., Payne, V. H., and Clarisse, L.: TES ammonia retrieval strategy and global observations of the spatial and seasonal variabiity of ammonia, Atmos. Chem. Phys., 11, 16 023–16 074, 2011.

Slattery, W. and Ronnfeldt, G.: Seasonal variation of pH, aluminium, and manganese in acid soils from north-eastern Victoria, Australian Journal of Experimental Agriculture, 32, 1105–1112, 1992.

Streets, D., Zhang, Q., Wang, L., He, K., Hao, J., Wu, Y., Tang, Y., and Carmichael, G.: Revisiting China's CO emissions after the Transport and Chemical Evolution over the Pacific (TRACE-P) mission: Synthesis of inventories, atmospheric modeling, and observations, J. Geophys. Res, 111, D14306, doi:10.1029/2006JD007118, 2006.

Streets, D. G., Bond, T. C., Carmichael, G. R., Fernandes, S. D., Fu, Q., Klimont, Z., Nelson, S. M., Tsai, N. Y., Wang, M. Q., Woo, J.-H., and Yarber, K. F.: An inventory of gaseous and primary aerosol emissions in Asia in the year 2000, J. Geophys. Res, 108, 8809, doi:10.1029/2002JD003093, 2003.

Sutton, M., Burkhardt, J., Guerin, D., Nemitz, E., and Fowler, D.: Development of resistance models to describe measurements of bi-directional ammonia surface-atmosphere exchange, Atmos. Environ., 32, 473–480, 1998.

Sutton, M. A., Nemitz, E., Erisman, J. W., Beier, C., Bahl, K. B., Cellier, P., de Vries, W., Cotrufo, F., Skiba, U., Di Marco, C., Jones, S., Laville, P., Soussana, J. F., Loubet, B., Twigg, M., Famulari, D., Whitehead, J., Gallagher, M. W., Neftel, A., Flechard, C. R., Herrmann, B., Calanca, P. L., Schjoerring, J. K., Daemmgen, U., Horvath, L., Tang, Y. S., Emmett, B. A., Tietema, A., Penuelas, J., Kesik, M., Brueggemann, N., Pilegaard, K., Vesala, T., Campbell, C. L., Olesen, J. E., Dragosits, U., Theobald, M. R., Levy, P., Mobbs, D. C., Milne, R., Viovy, N., Vuichard, N., Smith, J. U., Smith, P., Bergamaschi, P., Fowler, D., and Reis, S.: Chal-

lenges in quantifying biosphere-atmosphere exchange of nitrogen species, Environ. Pollut., 150, 125–139, doi:10.1016/J.Envpol.2007.04.014, 2007.

Van Damme, M., Clarisse, L., Heald, C. L., Hurtmans, D., Ngadi, Y., Clerbaux, C., Dolman, A. J., Erisman, J. W., and Coheur, P. F.: Global distributions and trends of atmospheric ammonia (NH_3) from IASI satellite observations, Atmos. Chem. Phys., 13, 24 301– 24 342, doi:10.5194/acp-14-2905-2014, 2014.

van der Werf, G. R., Randerson, J. T., Giglio, L., Collatz, G. J., Mu, M., Kasibhatla, P. S., Morton, D. C., DeFries, R. S., Jin, Y., and van Leeuwen, T. T.: Global fire emissions and the contribution of deforestation, savanna, forest, agricultural, and peat fires (1997-2009), Atmos. Chem. Phys., 10, 11 707–11 735, doi:10.5194/acp-10-11707-2010, 2010.

van Donkelaar, A., Martin, R. V., Leaitch, W. R., Macdonald, A. M., Walker, T. W., Streets, D. G., Zhang, Q., Dunlea, E. J., Jimenez, J. L., Dibb, J. E., Huey, L. G., Weber, R., and Andreae, M. O.: Analysis of aircraft and satellite measurements from the Intercontinental Chemical Transport Experiment (INTEX-B) to quantify long-range transport of East Asian sulfur to Canada, Atmos. Chem. Phys., 8, 2999–3014, doi:10.5194/acp-8-2999-2008, 2008.

Vestreng, V. and Klein, H.: Emission data reported to UNECE/ EMEP. Quality assurance and trend analysis and Presentation of WebDab, Norwegian Meteorological Institute, Oslo, Norway, MSC-W Status Report, 2002.

Walker, J. M., Philip, S., Martin, R. V., and Seinfeld, J. H.: Simulation of nitrate, sulfate, and ammonium aerosols over the United States, Atmos. Chem. Phys., 12, 11 213–11 227, doi:10.5194/acp-12-11213-2012, 2012.

Wang, Y., Zhang, Q. Q., He, K., Zhang, Q., and Chai, L.: Sulfate-nitrate-ammonium aerosols over China: response to 2000-2015 emission changes of sulfur dioxide, nitrogen oxides, and ammonia, Atmos. Chem. Phys., 13, 2635–2652, doi:10.5194/acp-13-2635-2013, 2013.

Wesely, M. L.: Parameterization of surface resistances to gaseous dry deposition in regional-scale numerical-models, Atmos. Environ., 23, 1293–1304, 1989.

Wichink Kruit, R. J., Schaap, M., Sauter, F. J., van Zanten, M. C., and van Pul, W. A. J.: Modeling the distribution of ammonia across Europe including bi-directional surface–atmosphere exchange, Biogeosciences, 9, 5261–5277, doi:10.5194/bg-9-5261-2012, 2012.

Xu, X., Wang, J., Henze, D. K., Qu, W., and Kopacz, M.: Constraints on aerosol sources using GEOS-Chem adjoint and MODIS radiances, and evaluation with multisensor (OMI, MISR) data, J. Geophys. Res. Atmos., 118, doi:10.1002/jgrd.50515, 2013.

Yevich, R. and Logan, J. A.: An assessment of biofuel use and burning of agricultural waste in the developing world, Global Biogeochem. Cycles, 17, 1095, doi:10.1029/2002GB001952, 2003.

Zhang, L., Wright, L. P., and Asman, W. A. H.: Bi-directional air- surface exchange of atmospheric ammonia: A review of measurements and a development of a big leaf model for applications in regional-scale air-quality models, J. Geophys. Res., 115, D20310, doi:10.1029/2009JD013589, 2010.

Zhang, L., Jacob, D. J., Knipping, E. M., Kumar, N., Munger, J. W., Carouge, C. C., van Donkelaar, A., Wang, Y. X., and Chen, D.: Nitrogen deposition to the United States: distribution, sources, and processes, Atmospheric Chemistry and Physics, 12, 4539–4554, doi:10.5194/acp-12-4539-2012, 2012.

Zhu, L., Henze, D. K., Cady-Pereira, K. E., Shephard, M. W., Luo, M., Pinder, R. W., Bash, J. O., and Jeong, G.: Constraining U.S. ammonia emissions using TES remote sensing observations and the GEOS-Chem adjoint model, J. Geophys. Res. Atmos., 118, doi:10.1002/jgrd.50166, 2013.

Zhu, L., Henze, D. K., Bash, J. O., Cady-Pereira, K. E., Shephard, M. W., Luo, M., and Capps, S. L.: Sources and impacts of atmospheric NH_3: Current understanding and frontiers for modeling, measurements, and remote sensing in North America, Current Pollution Reports,, doi:10.1007/s40726-015-0010-4, 2015.

Table 1. A summary of various emissions inventories used in different sections.

Section	Region	Horizontal	Model	Anthropogenic Emissions	Gross emissions in Region (Tg)		
		Resolution	Version	Inventory	April	July	October
4.2	US[a]	1/2 °× 2/3°	Static & Dynamic	NEI 2005[b]	0.200	0.407	0.223
4.3	Global	2°× 2.5°	Static & Dynamic	MASAGE_NH3[c]	6.79	6.59	5.01
6.1.1 6.1.2	US	1/2 °× 2/3°	BASE[d]	NEI 2005	0.200	0.407	0.223
			BIDI[d]	NEI 2005 livestock + upward BIDI flux[e]	0.153	0.428	0.192
6.1.3	US	2°× 2.5°	BASE	Optimized emissions inventories[f]	1.04	1.11	1.27
			BIDI		1.12	1.21	1.40
6.2 6.3 6.4	Global	2°× 2.5°	BASE	MASAGE_NH3	6.79	6.59	5.01
			BIDI		5.62	6.30	4.73

[a] Continental US.

[b] NEI 2005 does not distinguish the livestock emissions sector. Thus, the livestock fractions calculated from NEI 2008 are used in Dynamic case.

[c] MASAGE_NH3 contains livestock and fertilizer sectors.

[d] All BASE and BIDI cases include the new Dynamic scheme.

[e] In all BIDI cases, fertilizer emissions in BASE case will be replaced by the upward BIDI flux.

[f] Optimized emissions inventories from Zhu et al. (2013).

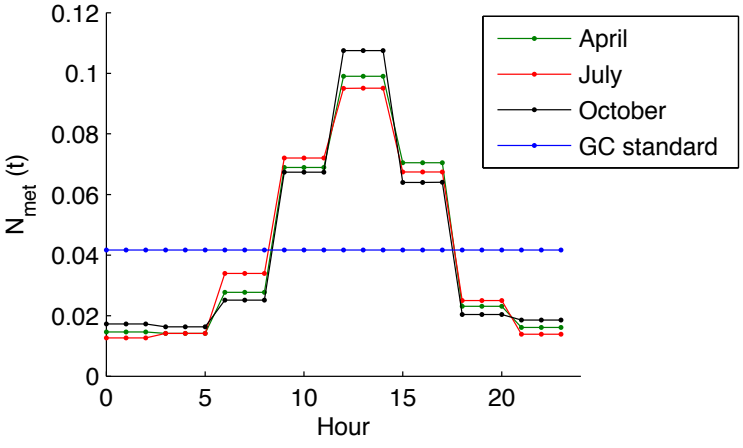

Figure 1. Monthly averaged diurnal variation fractions of livestock emissions of year 2008 over the US. Blue line is the standard GEOS-Chem. Dark green, red and black lines are the newly developed diurnal pattern of NH_3 livestock emissions in April, July and October, respectively.

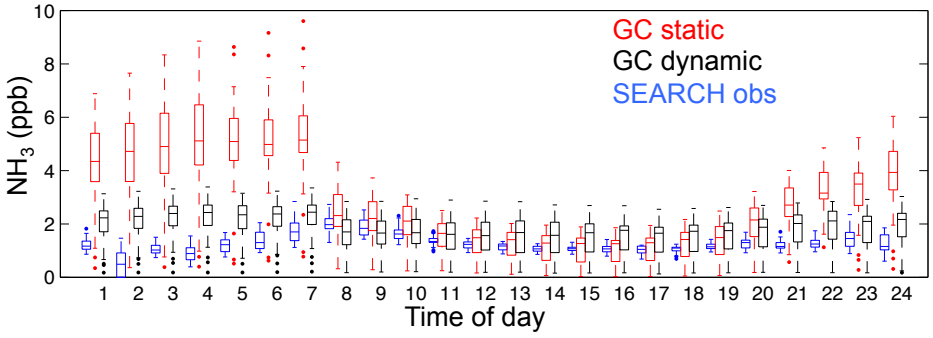

Figure 2. Diurnal variation of NH_3 surface concentrations from SEARCH observations (blue), GEOS-Chem model with (black) and without (red) dynamic emissions scheme in July 2008.

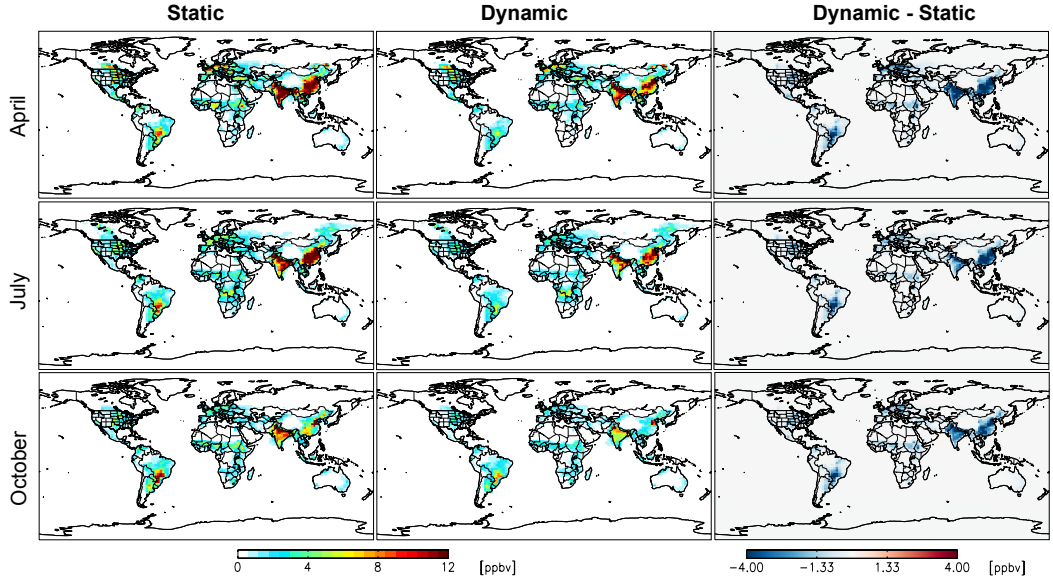

Figure 3. Spatial distribution of GEOS-Chem simulated NH_3 concentration at surface level in static, dynamic cases and their differences. Monthly averages are shown for April, July and October of 2008.

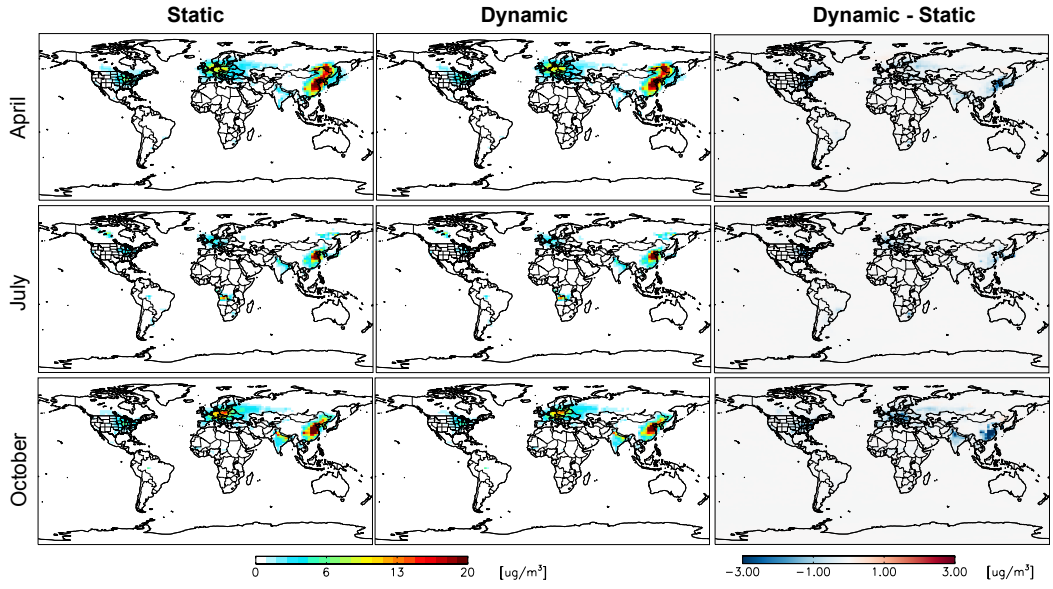

Figure 4. Spatial distribution of GEOS-Chem simulated nitrate concentration at surface level in static, dynamic cases and their differences. Monthly averages are shown for April, July and October of 2008.

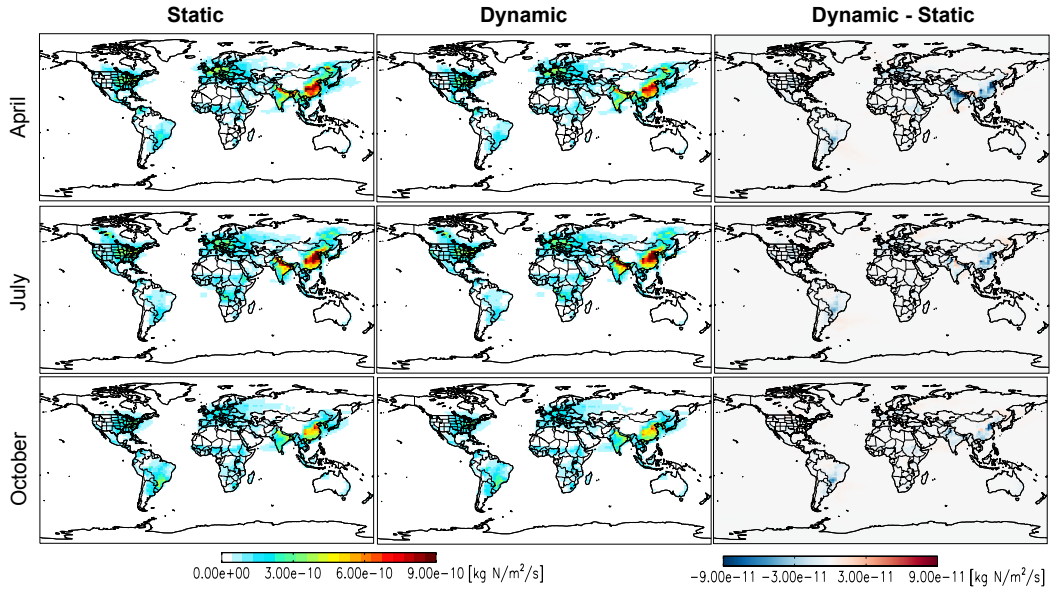

Figure 5. Spatial distribution of GEOS-Chem simulated total N deposition in static, dynamic cases and their differences. Monthly averages are shown for April, July and October of 2008.

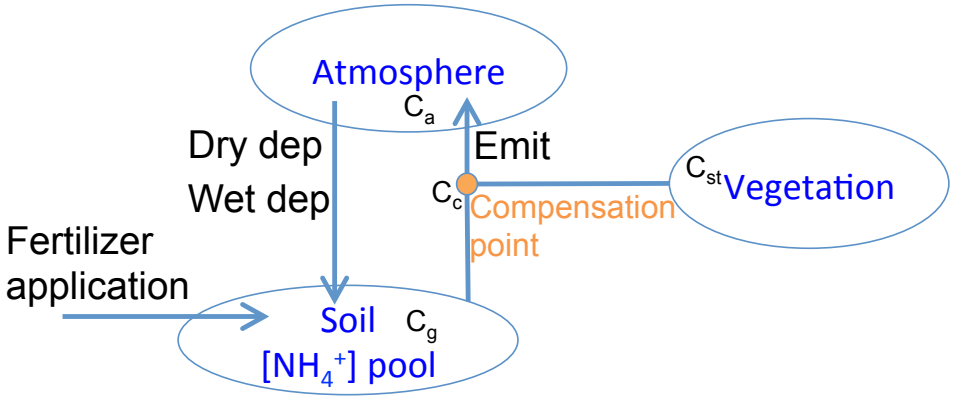

Figure 6. Simplified schematic of NH_3 bi-directional exchange model. C_a, C_g, C_{st} are the NH_3 concentrations in the atmosphere, soil and stomata, respectively. C_c is the NH_3 concentration at the canopy compensation point.

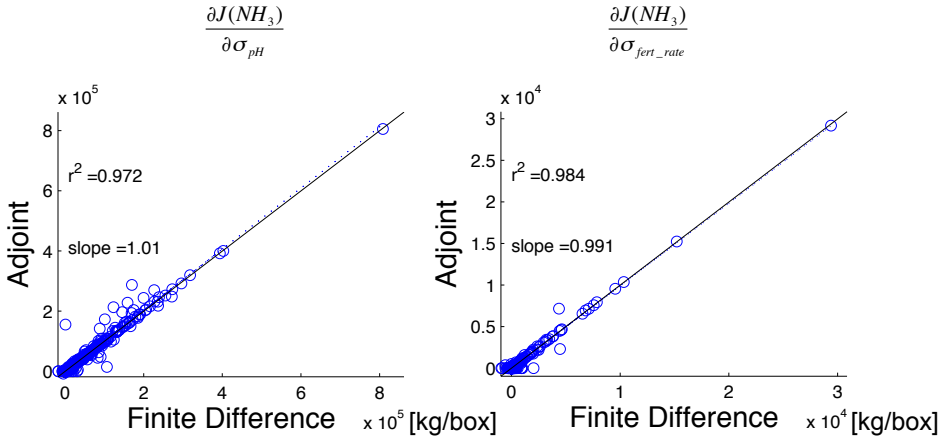

Figure 7. The adjoint sensitivity of NH_3 surface level concentration with respect to soil pH (left) and fertilizer application rate (right) compared to finite difference gradients. The cost function is evaluated once at the end of a one week simulation which excludes horizontal transport.

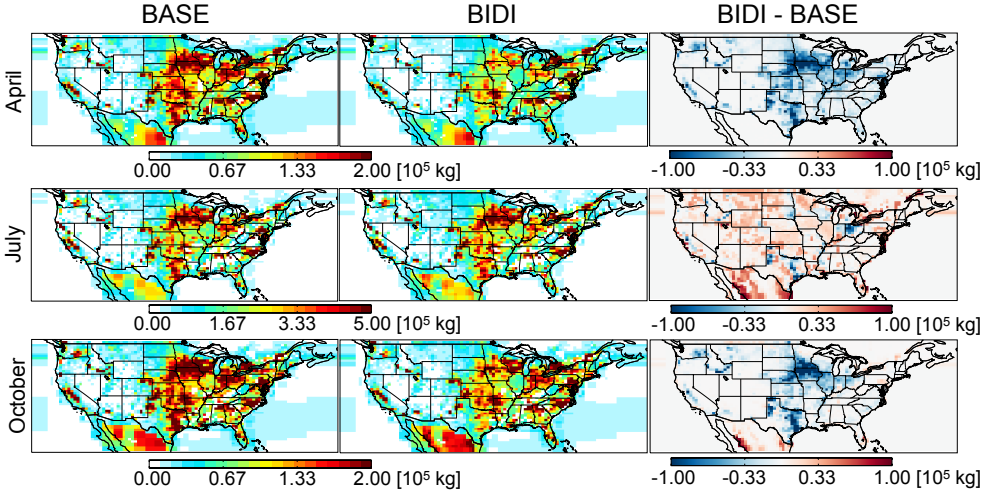

Figure 8. Spatial distribution of ammonia total emissions from GEOS-Chem with (BIDI) and without (BASE) bi-directional exchange and their differences in April, July and October of 2008. The total emissions in the BIDI case are the sum of upward fluxes from soil and vegetation from the bi-directional exchange and emissions from all other sources except fertilizers.

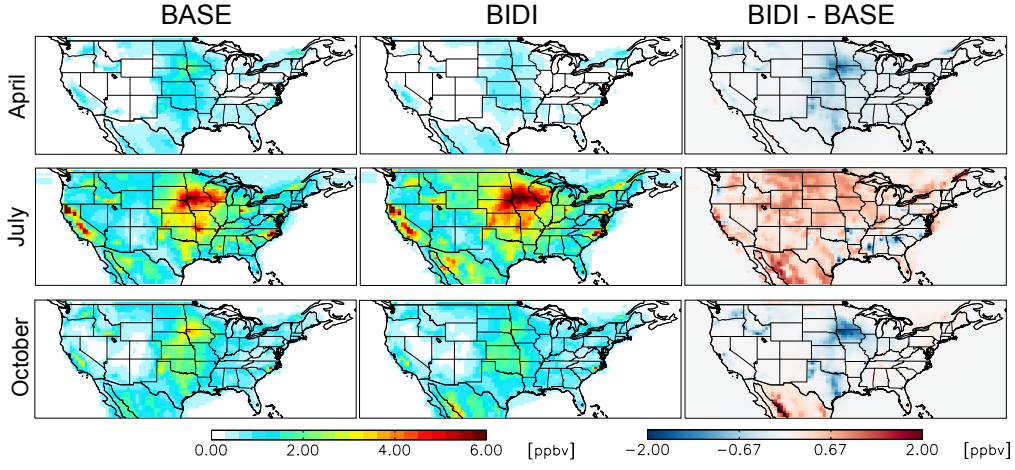

Figure 9. Spatial distribution of ammonia concentration at surface level of GEOS-Chem with (BIDI) and without (BASE) bi-directional exchange and their differences in April, July and October of 2008.

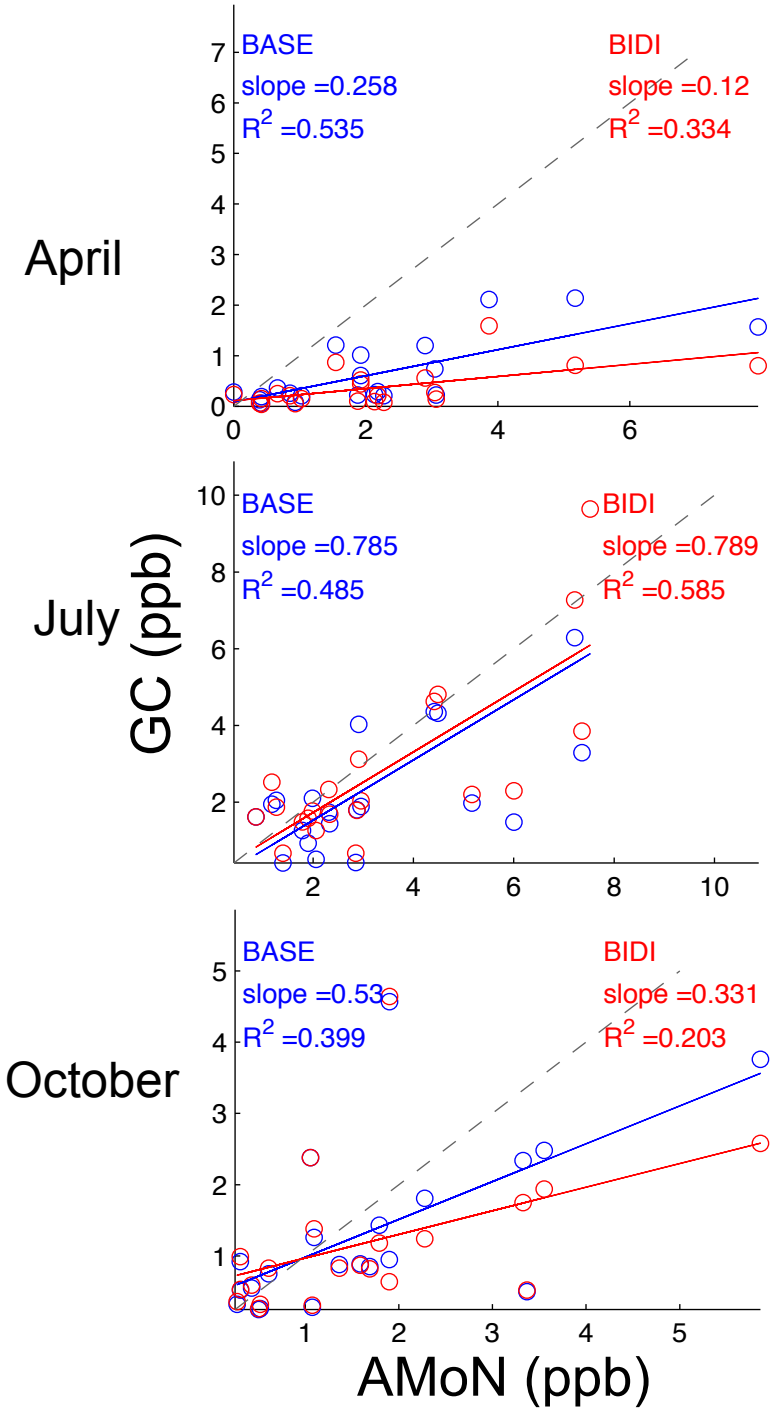

Figure 10. Comparison of GEOS-Chem simulated NH_3 concentration at surface level in BASE and BIDI cases with AMoN observations in April, July, and October of 2008. R^2 is the square of the correlation coefficient. Solid lines are regressions. Gray dashed lines are 1:1.

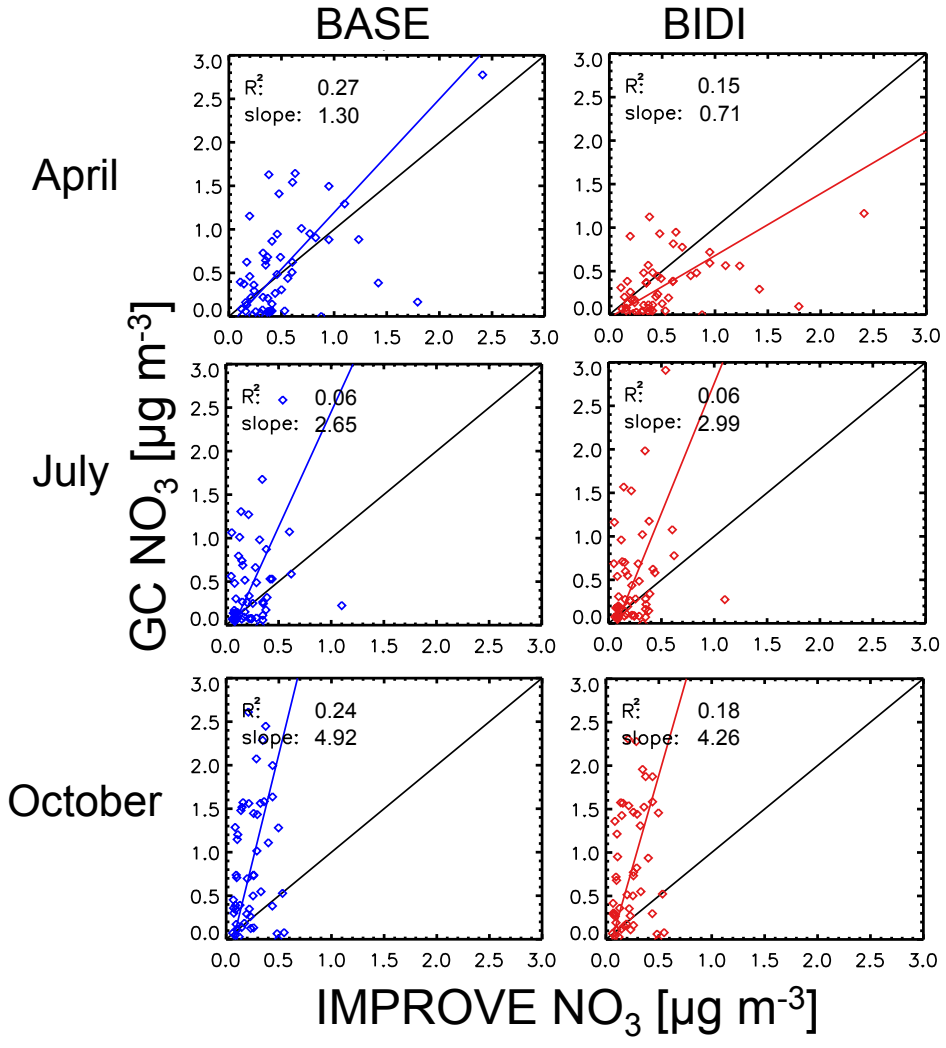

Figure 11. Comparison of GEOS-Chem simulated nitrate aerosol concentration at surface level in BASE and BIDI cases with IMPROVE observations in April, July, and October of 2008. R is the correlation coefficient.

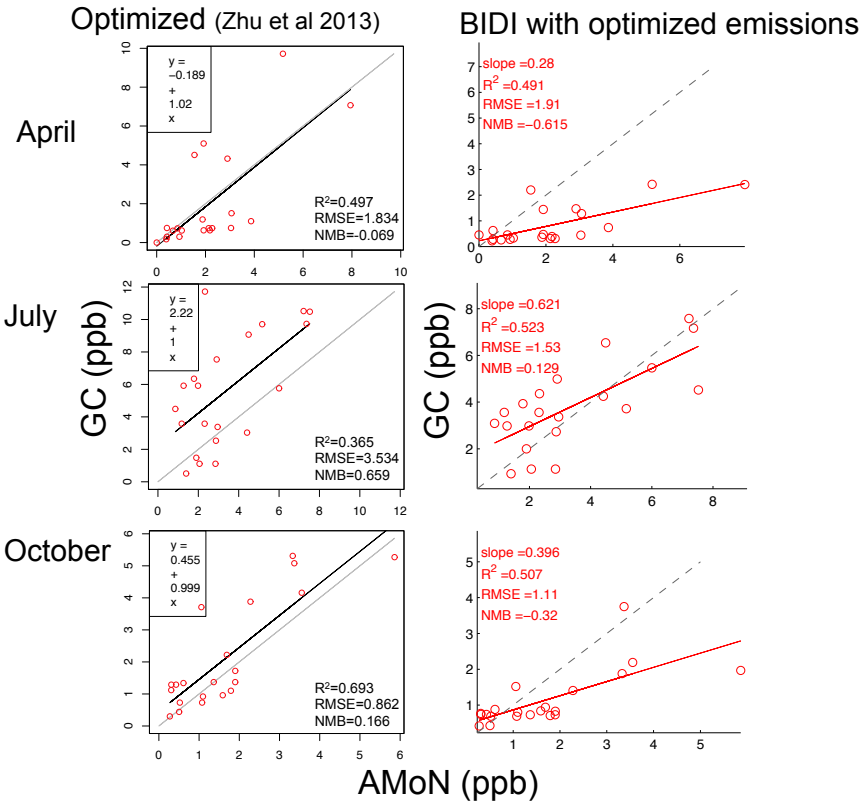

Figure 12. Left column: comparison of GEOS-Chem optimized NH_3 concentration at surface level from Zhu et al. (2013) with AMoN observations. Right column: comparison of GEOS-Chem simulated NH_3 concentration at surface level in BIDI case using optimized NH_3 emissions from Zhu et al. (2013) with AMoN observations. R^2 is the square of the correlation coefficient. Gray dashed lines are 1:1.

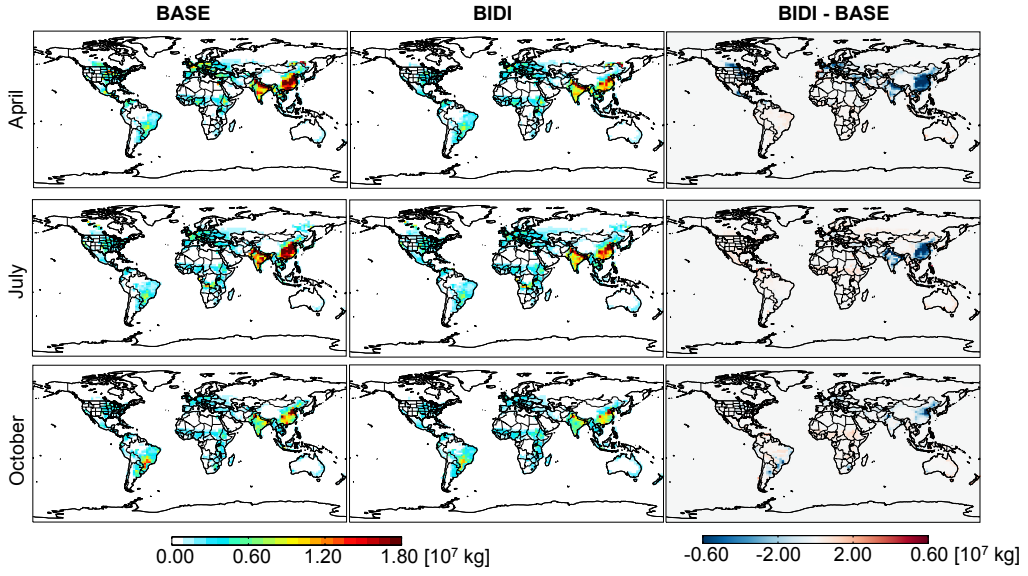

Figure 13. Global distribution of ammonia gross emissions from GEOS-Chem with (BIDI) and without (BASE) bi-directional exchange and their differences in April, July and October of 2008. The total emissions in the BIDI case are the sum of upward fluxes from soil and vegetation from the bi-directional exchange and emissions from all other sources except fertilizers.

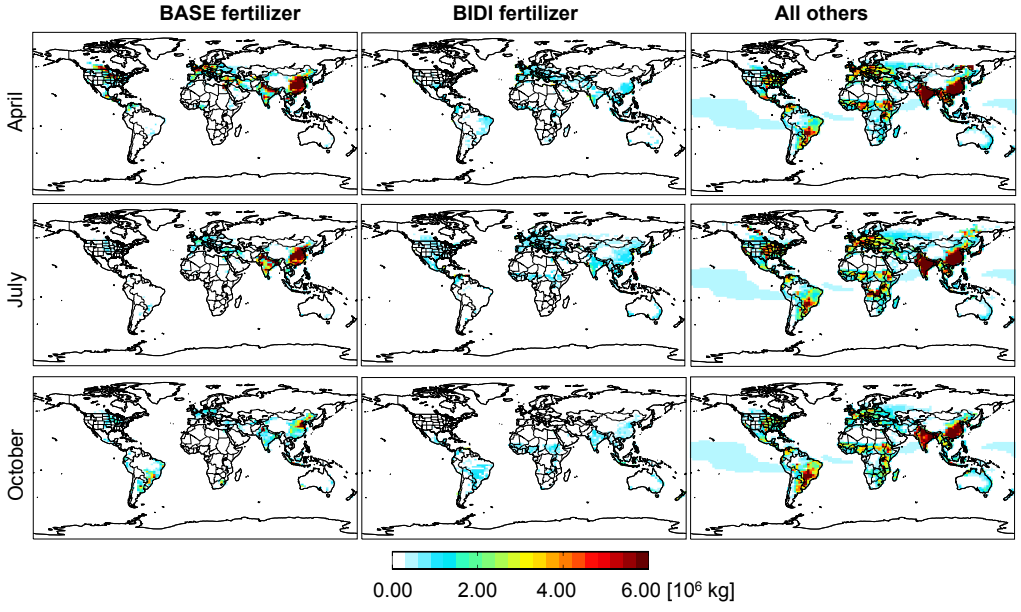

Figure 14. Global distribution of original ammonia fertilizer emissions in BASE case (BASE fertilizer), upward flux from soil and vegetation in BIDI case (BIDI fertilizer), and ammonia emissions from all other sources except fertilizers (All others) in April, July and October of 2008.

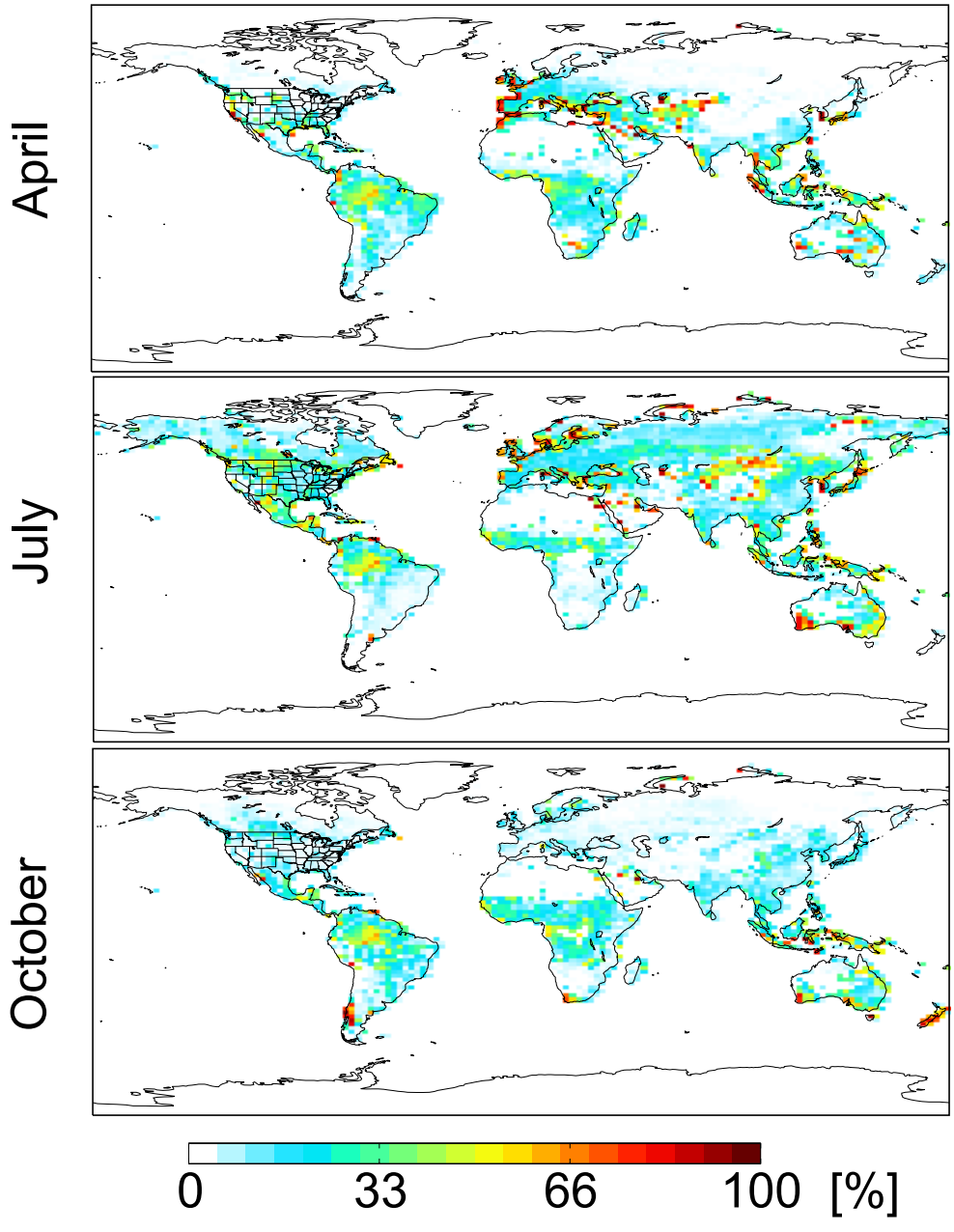

Figure 15. Percentage of gross emissions owing to fertilizer in the global BIDI case in April, July and October of 2008.

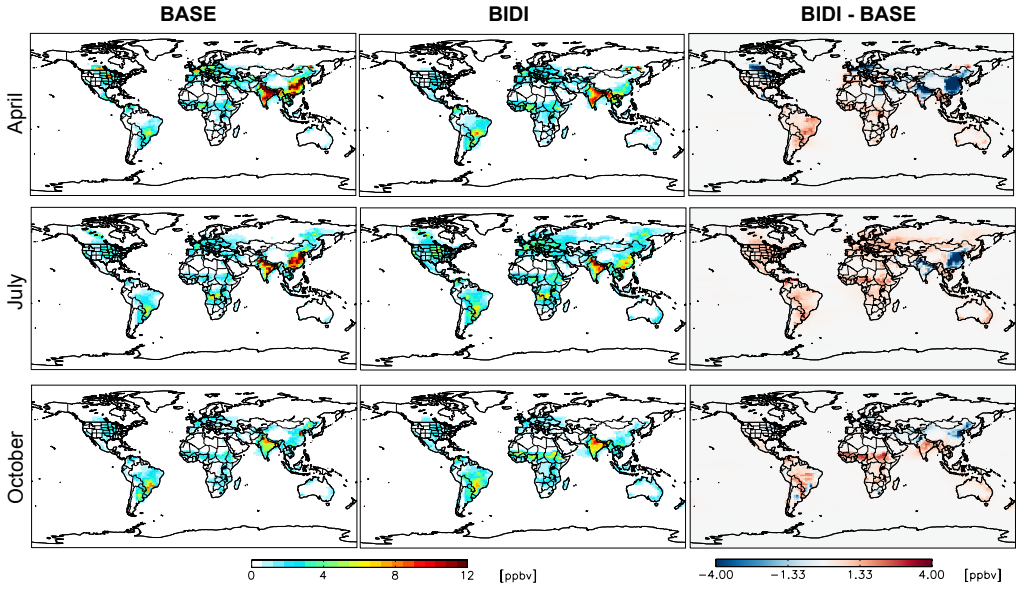

Figure 16. Global distribution of ammonia concentration at surface level of GEOS-Chem with (BIDI) and without (BASE) bi-directional exchange and their differences in April, July and October of 2008.

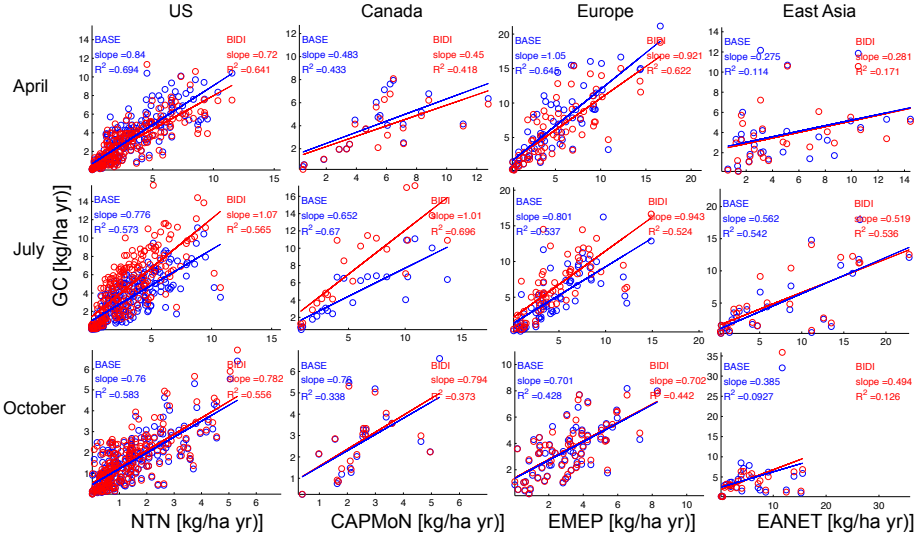

Figure 17. Comparisons of GEOS-Chem modeled NH_4^+ wet deposition in BASE (blue) and BIDI (red) cases with in situ observations in US (1st column), Canada (2nd column), Europe (3rd column), and East Asia (4th column) in April (1st row), July (2nd row), and October (3rd row) of 2008. The y-axis represent the model values, and the x-axis represent observations from NTN (for US), CAPMoN (for Canada), EMEP (for Europe), EANET (for East Asia). R^2 is the square of the correlation coefficient.

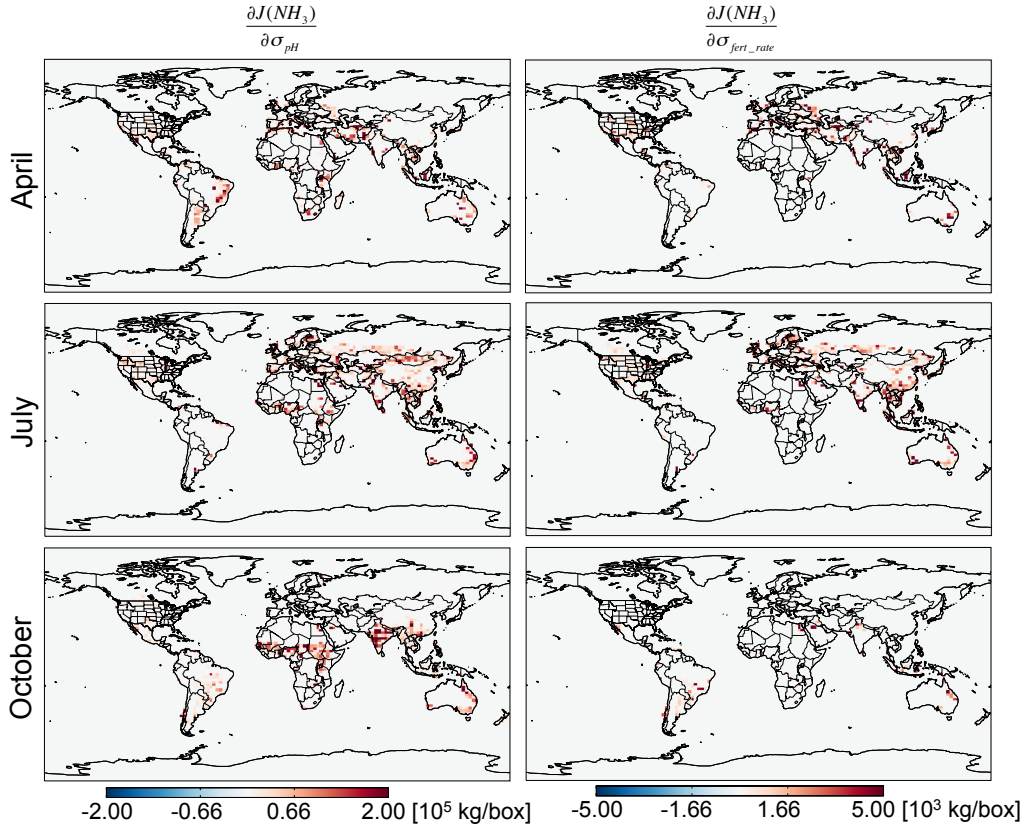

Figure 18. The adjoint sensitivities of NH_3 surface level concentration with respect to soil pH scaling factor (left) and fertilizer application rate scaling factor (right) in April, July, and October of 2008. Note that sensitivities in the left and right columns have different scales.

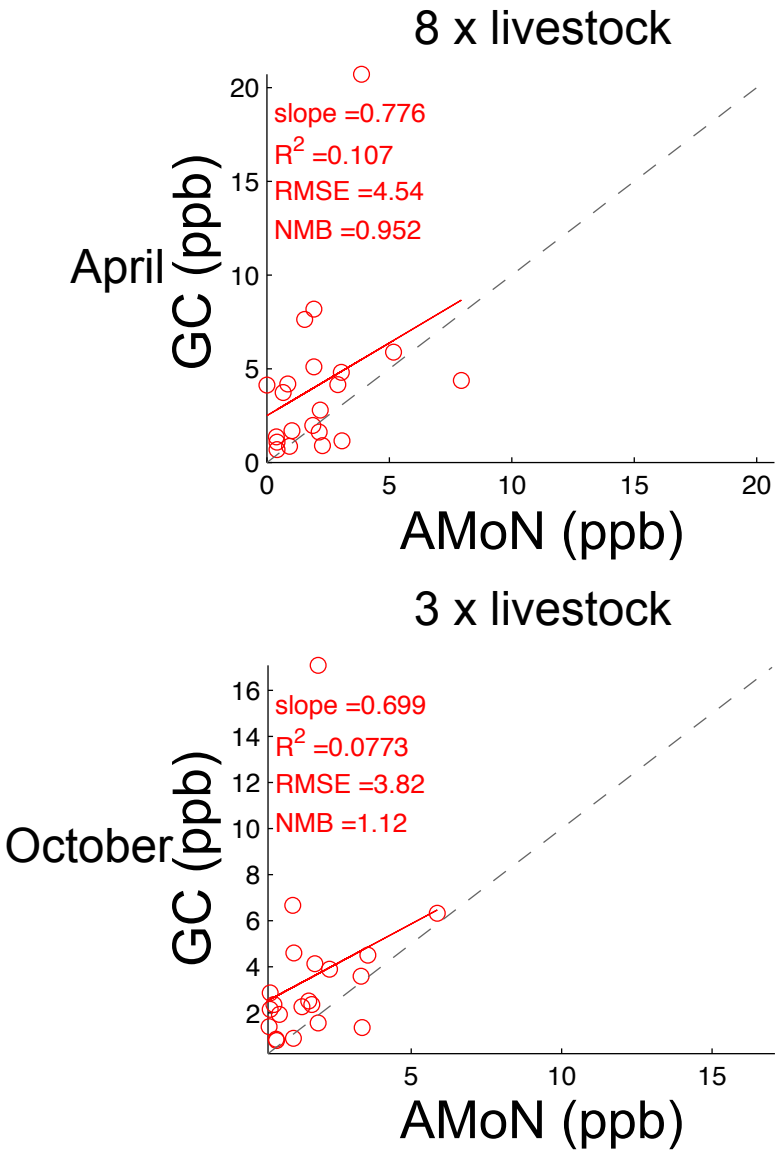

Figure 19. Comparison of NH_3 surface concentrations from GEOS-Chem with bi-directional exchange to AMoN observations. The livestock emissions in the model are increased by a factor of 6 in April, and 3 in October.

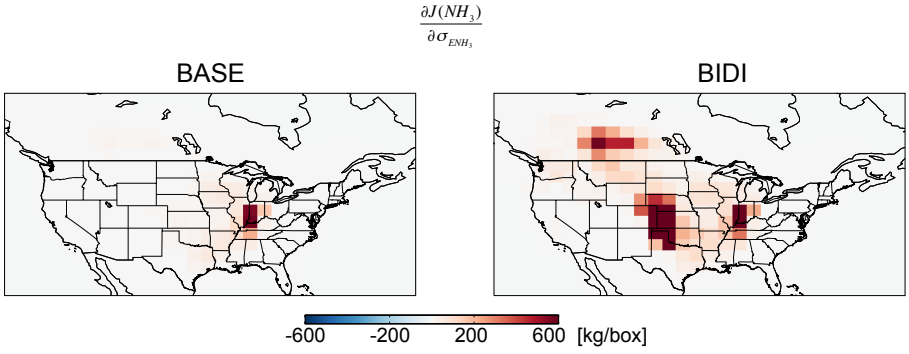

Figure 20. The adjoint sensitivities of NH_3 surface level concentration at 88°W, 40°N with respect to NH_3 anthropogenic emission scaling factor at all grid cells in both BASE (left) and BIDI (right) cases in April, 2008.